EXAMINATION OF THE ASSOCIATION BETWEEN ARTERIAL BLOOD PRESSURE BELOW THE LOWER LIMIT OF AUTOREGULATION AND ACUTE KIDNEY INJURY AFTER CARDIAC SURGERY

by
Rohan Nadkarni

A thesis submitted to Johns Hopkins University in conformity with the requirements for the degree of Master of Science in Engineering

Baltimore, Maryland
May 2019

Abstract

Acute kidney injury (AKI) is common among cardiac surgery patients. Although there are many

causes of AKI, an important contributor is a reduction in arterial blood pressure (ABP).

However, there are no clear guidelines on the minimum ABP required during surgery, and this

value may vary between patients. Researchers have hypothesized that cerebral autoregulation

monitoring could provide useful information to address this problem, with the assumption that

maintaining ABP above the minimum value required for perfusion to the brain (the lower limit of

autoregulation (LLA)) would also ensure perfusion to the kidneys. In support of this hypothesis,

a previous study found an association between ABP below the LLA and AKI. Unfortunately,

there are limitations to this body of research, including poor scalability of methods, few clinical

studies, and assumptions in choosing parameters to quantify ABP below the LLA.

      This thesis addresses the limitations of prior autoregulation research. The initial steps

were to develop an algorithm for automated LLA selection and to test its accuracy. This

algorithm was used to analyze the strength of association between ABP below the LLA and AKI

in a recent patient population. Finally, sensitivity analyses were performed to examine

assumptions in quantifying ABP below the LLA.

      The algorithm's primary method of LLA selection (threshold crossing) was accurate

compared to expert adjudication. A secondary method (parabola fit) appeared to be useful in

identifying an LLA in additional patients but could not be validated. Using the primary method,

prior findings of an association between AKI and area of the ABP curve below the LLA (AUC)

were reproduced in a new cohort. Sensitivity analyses demonstrated that time below LLA had a comparable strength of association with AKI, the optimal COx threshold appeared to be 0.325, and an association between AUC and AKI was absent in patients with reduced kidney function but was strong in patients with normal kidney function. These results support an association between ABP below the LLA and AKI and suggest that further studies to determine whether maintaining ABP above the LLA can reduce the risk of AKI are warranted, particularly in patients with normal kidney function.

Primary Reader: Charles Brown

Secondary Readers: Archana Venkataraman, Brian Bush

Contents

List of Tables

List of Figures

Chapter 1

Introduction

1.1. Purpose of Research

Acute kidney injury (AKI) is common in cardiac surgery patients, with an estimated incidence of 5-30 percent [1]. Management of modifiable factors that are known to be associated with AKI is critical to its prevention. Although there are many potential causes of AKI, an important contributor in the perioperative period is a reduction in arterial blood pressure (hypotension) that results in decreased blood flow, so that the kidneys become damaged due to an insufficient supply of oxygen (ischemia) [2]. In particular, cardiopulmonary bypass involves low blood pressure and blood flow that is not driven by the heartbeat, so patients who undergo this procedure are at high risk of developing AKI [2].

Unfortunately, there are no clear guidelines for avoiding hypotension-induced ischemia, since the definition of hypotension is not well established for individual patients. In fact, a systematic review reported over 100 different definitions of intraoperative hypotension in the anesthesia literature [3]. To address this problem, our research team at Johns Hopkins has examined whether measurement of cerebral autoregulation could provide further insight, with the underlying assumption that maintaining blood pressure above that required for perfusion to the brain will also ensure perfusion to the kidneys and prevent ischemia.

Cerebral autoregulation is the process by which the cerebral blood vessels constrict or dilate in response to changes in arterial blood pressure (ABP) so that cerebral blood flow (CBF) remains relatively constant [4]. However, when ABP falls below a certain value, CBF passively changes with ABP, elevating the risk of ischemia [5]. This critical pressure value is called the lower limit of autoregulation (LLA) [5]. Since the body has evolved to maintain CBF through autoregulation, we hypothesized that the cerebral LLA will serve as a surrogate for minimal blood pressure to the kidneys. Indeed, in an observational study of 410 patients, Ono et al. demonstrated a statistically significant association between ABP below the LLA and AKI [1]. Unfortunately, there are several limitations to this body of research, which include poor scalability of methods, a relatively small number of clinical studies, and assumptions in choosing key parameters to quantify ABP below the LLA.

This thesis attempts to address some of the concern related to past research. First, to make LLA selection automated, we designed an algorithm that uses mathematical rules based on the input of expert clinicians for LLA selection. Second, we used this algorithm to test whether the findings reported by Ono et al. can be replicated in a population of recent cardiac surgery patients [1]. Third, we explored how modifying the method of quantifying ABP below the LLA, changing parameter settings for computing the LLA, and stratifying by baseline kidney function would affect the association with AKI. These analyses are meant to reveal the strongest associations between ABP below the LLA and AKI in order to help maximize the utility of autoregulation monitoring in reducing the occurrence of AKI.

1.2. Background

1.2.1. Acute Kidney Injury

Acute kidney injury (AKI) refers to a rapid deterioration of kidney function, leading to the retention of fluid and waste products in the bloodstream [6]. AKI is linked to several undesirable outcomes, including excess fluid in the lungs and limbs, weak muscles, irreversible kidney damage, and death [6]. In cardiac surgery patients, AKI inhibits recovery, with severe cases requiring the use of dialysis [7, 8]. Furthermore, cardiac surgery patients with AKI have an elevated risk of death during the hospital stay [7]. There are 3 main categories of AKI based on origin of the injury: pre-renal, intrinsic, and post-renal [9]. Pre-renal AKI refers to a decrease in glomerular filtration rate (GFR) caused by inadequate renal blood flow, and treatment can involve either correction of blood volume depletion or use of vasopressors to increase blood pressure, depending on the specific circumstances [9, 10, 11]. Intrinsic renal AKI often involves direct injury to the tubules, glomeruli, interstitium, or intra-renal blood vessels [9]. This type of AKI can be diagnosed with urine sediment tests, blood tests, or biopsy, and treatment may involve steroid therapy or ceasing use of certain drugs [11]. In post-renal AKI, obstructed flow of urine results in greater intra-tubular pressure that decreases GFR [9]. In many cases, this obstruction is corrected by surgical removal of tumors or kidney stones [11].

The criteria for diagnosing AKI have changed over time, but have consistently relied on serum creatinine (SCr) and urine output (UO) [9]. The first widely accepted diagnosis method was the Risk Injury Failure Loss End-Stage Renal Disease (RIFLE) criteria. The RIFLE criteria classify severity of AKI into three stages: Risk, Injury, and Failure. These stages are based on

changes in SCr and UO from baseline levels [9]. In addition, these criteria define two stages of outcome, Loss and End-Stage Renal Disease, that are based on the length of time that kidney function remains impaired [9]. The most recent diagnostic standards are known as Kidney Disease: Improving Global Outcomes (KDIGO). Like RIFLE, these standards divide AKI into 3 stages of severity, where Stage 1 represents risk of AKI and Stage 3 represents kidney failure, and classify patients into these stages based on increases in SCr and decreases in UO [9]. A notable change is that Stage 1 of KDIGO examines percent increase in SCr over seven days as well as the absolute increase in SCr over two days, whereas the Risk stage of RIFLE only incorporates percent increase in SCr over seven days [9].

Since AKI is a common post-surgical complication, several strategies have been developed to reduce the frequency of this outcome. The KDIGO guidelines for surgery include maintaining sufficient blood pressure, careful monitoring of blood volume, avoiding use of nephrotoxic agents, temporarily ceasing use of angiotensin converting enzyme inhibitors (ACEi) and angiotensin II receptor blockers (ARBs), and preventing hyperglycemia in high risk patients [12]. This strategy was found to reduce AKI in a controlled trial [12].

While avoiding hypotension is likely a critical factor in preventing AKI during surgery, the target blood pressure for achieving this goal is uncertain, and the appropriate target may vary significantly from patient to patient. Thus, identifying an optimal arterial blood pressure to ensure adequate kidney perfusion is an important strategy to reduce the risk of postoperative AKI.

1.2.2. Cerebral Autoregulation

Overview

Cerebral autoregulation is the physiologic process for ensuring adequate CBF despite changes in ABP [4]. This function is automatically performed by the cerebral vasculature, which responds to changes in ABP through diameter changes that alter cerebrovascular resistance [4]. Autoregulation is largely mediated by the innate response of vascular smooth muscle, but also involves control from the autonomic nervous system and metabolic mechanisms [13].

The process of cerebral autoregulation was first described by Lassen and is depicted in Figure 1 (Lassen's curve) [14]. As seen in this curve, autoregulation keeps CBF relatively constant when ABP fluctuates between the lower limit of autoregulation (LLA) and the upper limit of autoregulation (ULA) [5]. However, when ABP falls below the LLA, CBF decreases with decreases in ABP, raising the risk of ischemia [5]. The idea of monitoring autoregulation in individual surgery patients has gained support in recent years, and there is growing evidence that the use of personalized ABP targets derived from patient-specific LLA values could potentially help prevent AKI and other undesirable effects of hypotension [15].
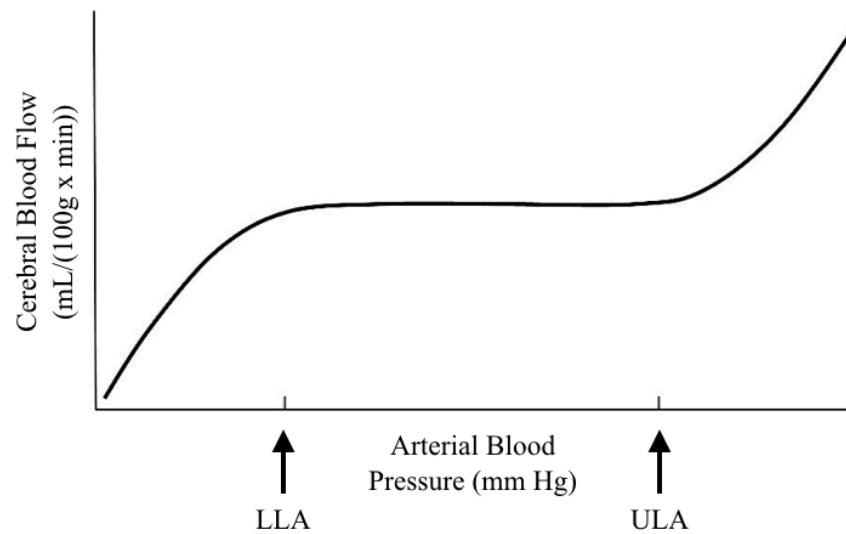
Figure 1: Classic Lassen's curve for cerebral autoregulation [14].

In pig models, cerebral autoregulation curves similar to Figure 1 have been generated using catheters to measure blood pressure and laser-Doppler to measure cerebral blood flow [16]. Since pig model research permits invasive intracranial pressure (ICP) measurement, these studies monitor cerebral perfusion pressure (CPP) instead of ABP [16]. Laser-Doppler measures red blood cell flux, which acts as a gold standard for CBF [16]. Using data from slow exsanguination of pigs, scatterplots of laser-Doppler flux versus CPP were generated. Then, two regression lines that minimized the combined residual squared error were fit to this data, and the CPP at the breakpoint between the two lines was identified as the LLA [16]. This process for LLA selection is displayed in Figure 2 [16].
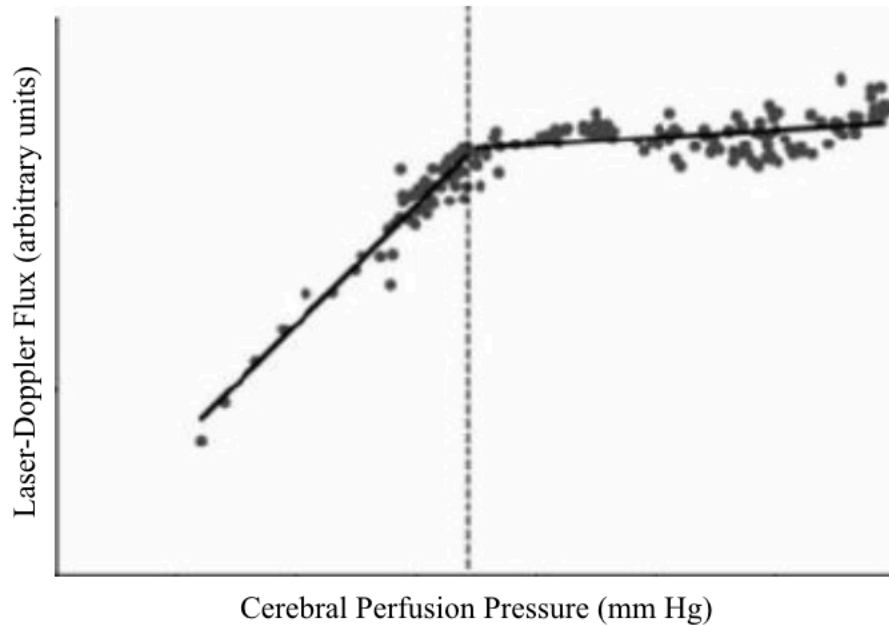
Figure 2: Scatter plot of laser-Doppler flux versus cerebral perfusion pressure in a pig [16]. The LLA is indicated by the CPP value at the breakpoint separating the two regression lines.

However, there are several limitations to identifying the LLA from a scatter plot that preclude its use in humans. First, data was only obtained after exsanguination of the pigs with a substantial amount of time spent at low cerebral perfusion pressure values [16]. Second, laser-Doppler cannot be routinely used to measure cerebral blood flow because it requires an invasive craniotomy, as illustrated in Figure 3 [16, 17]. In order to address these limitations, several approaches have been proposed to analyze the relationship between ABP and non-invasive surrogates of CBF. The two main categories of approaches are time-domain approaches, which interpret correlation between ABP and CBF, and frequency-domain approaches, which interpret

7

magnitude and phase of the transfer function between ABP and CBF [16, 18]. Both methods are discussed in the following section.
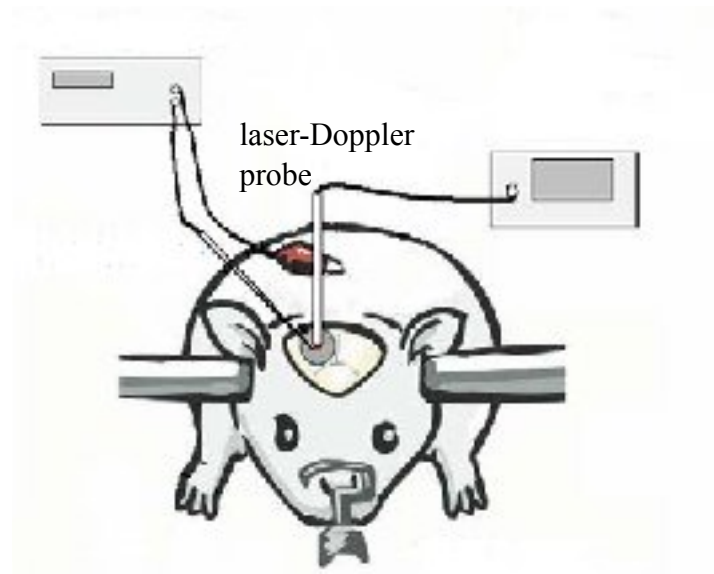
Figure 3: Diagram of laser-Doppler recording in a rat [17].

Real Time Monitoring of Cerebral Autoregulation: Time-Domain and Frequency-Domain Approaches

Time-domain approaches for monitoring cerebral autoregulation are based on linear correlation between ABP and a CBF surrogate [16]. Since the Lassen curve displays a positive linear relationship between ABP and CBF when ABP is outside of the limits of autoregulation and constant CBF when ABP is between the lower and upper limits, these approaches assume that a linear correlation coefficient near 0 indicates intact autoregulation while a correlation coefficient near 1 indicates autoregulation failure [19]. To calculate these correlations, both signals are first low-pass filtered with a moving average filter that computes the mean value in 10 second, non-

overlapping time windows [16]. This step removes respiratory and pulse frequencies while keeping the frequency data below 0.05 Hz that is relevant to autoregulation monitoring [16]. A high-pass filter is then applied to remove frequencies below 0.003 Hz [16]. Pearson's correlation coefficients between ABP and the CBF surrogate are computed in 300 second (30 point) overlapping windows [16]. The degree of overlap between consecutive correlation coefficient computations has varied in prior research, with some studies using 24 point overlap and others using 29 point overlap [16, 20]. The final signal processing step is to place each correlation coefficient data point into a bin of 5 mm Hg width according to the mean ABP in its 300 second window [16]. This results in an error bar plot that displays the mean and standard deviation of the correlation coefficient in each 5 mm Hg bin [16]. Based on pig models, the LLA is thought to occur where the mean correlation coefficient crosses from above to below approximately 0.3, as shown in Figure 4 [16].
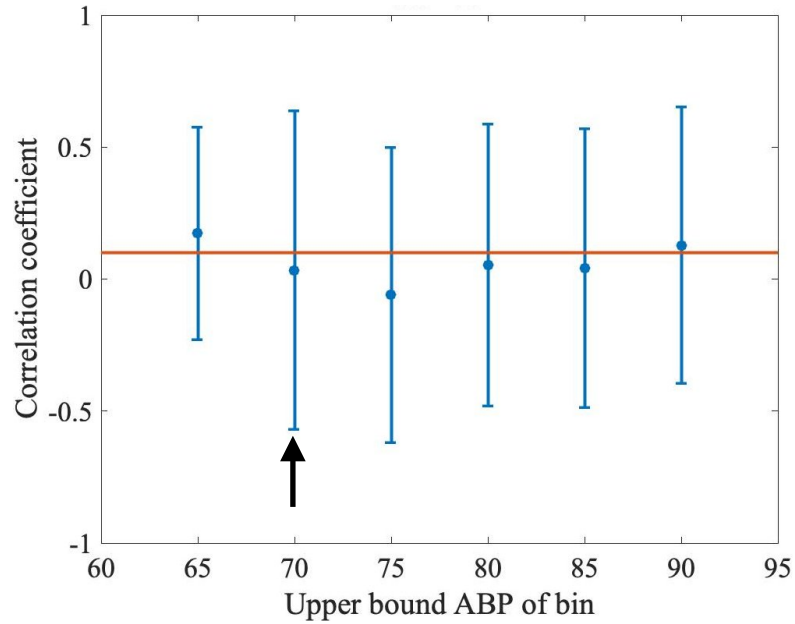
Figure 4: Example of error bar plot. A threshold line is drawn at 0.3. The arrow indicates the bin corresponding to the LLA.

Frequency domain approaches for monitoring cerebral autoregulation, such as those described in Blaber et al., analyze phase and gain of the transfer function between ABP and surrogates of CBF [18]. Examples of these plots are shown in Figure 5 [18]. A smaller gain of the transfer function at low frequencies (below 0.05 Hz) indicates that autoregulation is functioning because it means that the change in magnitude of CBF in response to changes in ABP is small [16, 18]. A zero degree phase shift in the transfer function at low frequencies means that ABP and CBF change in concert, indicating a lack of autoregulation [19]. A negative phase shift means that CBF changes before ABP does and indicates intact autoregulation [19]. While frequency-domain analysis does provide important information about the autoregulation response, it relies on the assumption that the statistical properties of ABP and CBF do not change

with time, which is not the case for patients undergoing cardiac surgery [21]. For this reason, time-domain methods are the focus of this thesis.
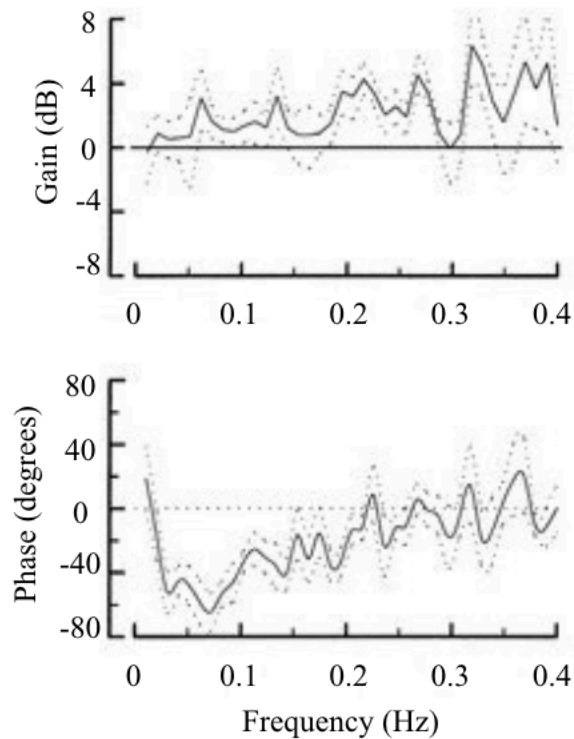
Figure 5: Examples of gain and phase of transfer function between ABP and CBF [18]. The low gain and negative phase at frequencies less than 0.05 Hz indicate intact autoregulation [16, 18, 19].

Measuring Surrogates for Cerebral Blood Flow

While laser-Doppler provides a reliable measurement of CBF, it requires a craniotomy so that the probe can be in direct contact with the frontoparietal cortex [16]. Due to the invasiveness of this method, use of laser-Doppler is not feasible in human patients and has therefore been limited to

animal studies [16]. A noninvasive alternative is flow velocity measurement with transcranial

Doppler (TCD), which is shown in Figure 6 [16, 22, 23]. However, TCD has several limitations,

such as the need for the transducer to be repeatedly repositioned and inability to consistently

obtain stable recordings [22].
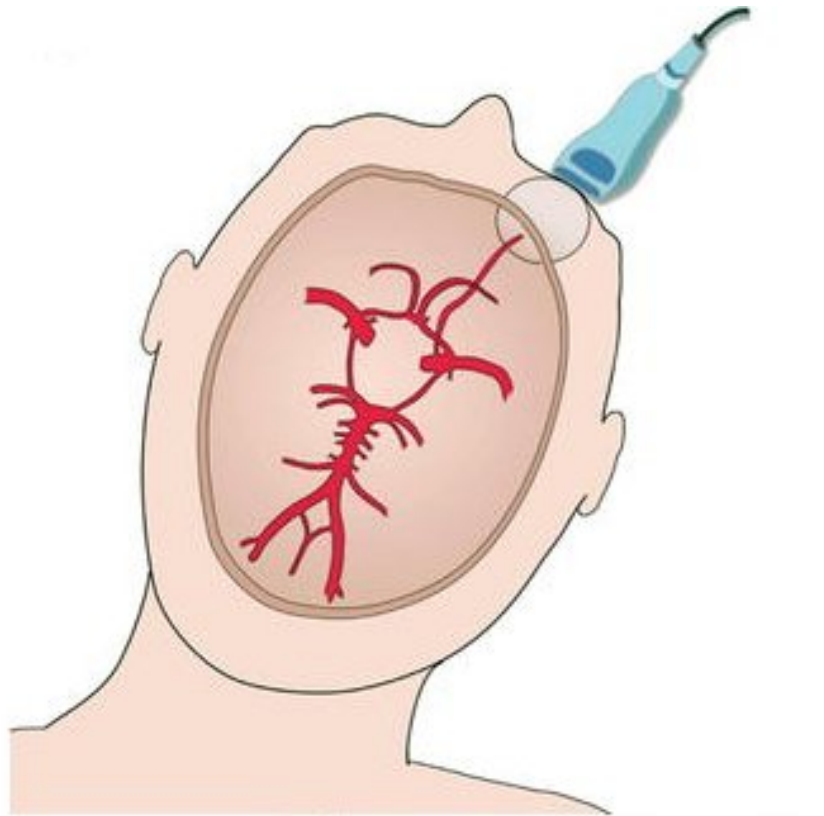
Figure 6: Diagram of transcranial Doppler recording in a human [23].

To address these limitations, near-infrared spectroscopy (NIRS) has been proposed as an

alternative surrogate for cerebral blood flow. NIRS is a non-invasive method that measures

cerebral tissue oxyhemoglobin saturation [16]. The main determinants of this value are cerebral

blood flow, hemoglobin concentration, arterial oxygen saturation, and brain metabolic rate [14].

It is often assumed that the latter three factors are constant over short times, so that NIRS may be

used as a surrogate of CBF [24]. In order to obtain NIRS measurements, an oximeter probe that

contains a light source and a detector is attached to the scalp [25]. The light source emits near-

infrared light, which is transmitted through the skull and reaches cerebral tissue [25].

Photodetectors in the probe detect the light that is reflected from the cerebral tissue back to the

probe on the scalp [25]. Using the Beer-Lambert law and the known absorption spectra of

oxygenated and deoxygenated hemoglobin, cerebral tissue oxyhemoglobin saturation is

calculated [25]. This recording procedure is illustrated in Figure 7 [26].
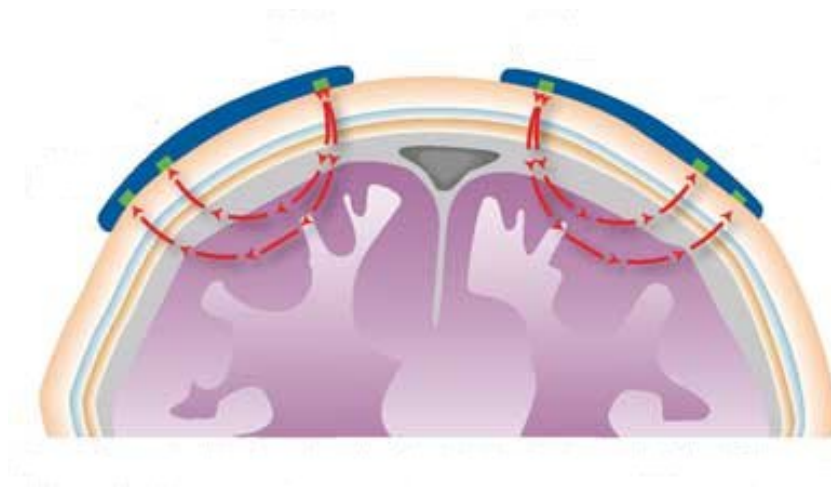
Figure 7: Diagram of near-infrared spectroscopy recording [26].

Validation of Time-Domain Cerebral Autoregulation Monitoring in Pigs

A significant challenge in monitoring autoregulation is to validate non-invasively obtained

information regarding cerebral autoregulation with gold-standard measurements that are only

available in animal models. Thus, Brady et al. utilized a pig model to compare time-domain

correlation approaches for determining the LLA to a Lassen's curve obtained with the gold

standard method shown in Figure 2 [16]. For this analysis, the correlation between CPP and laser-Doppler was calculated (laser-Doppler index (LDx)) and sorted into an error bar plot using the same general procedure described above for time-domain monitoring of autoregulation [16]. The LDx plots displayed a sharp drop in mean correlation coefficient at CPP values above the gold standard LLA, and thus the LDx coefficients appeared to provide meaningful information on autoregulation [16].

Because NIRS is a preferred choice for autoregulation monitoring in humans, a subsequent goal was to validate NIRS-based methods of monitoring autoregulation versus a gold standard in pigs [16]. Since an LLA cannot be obtained from piecewise linear regression in a scatterplot of NIRS versus CPP, as shown in Figure 8, autoregulation monitoring with NIRS could only be done using correlation approaches [16]. The error bar plot for correlation between CPP and NIRS, which is called the cerebral oximetry index (COx), was generated in a similar fashion to the LDx measure described above [16]. The COx error bar plot also displayed a sharp drop in mean correlation coefficient at CPP values above the gold standard LLA [16]. This demonstration of agreement between COx and LDx was an important step in the validation of NIRS as a useful tool for monitoring of autoregulation in the time domain. Additionally, it was noted that a COx of 0.36 appeared to delineate the ABP at the LLA, using the Lassen curve as a gold standard [16].
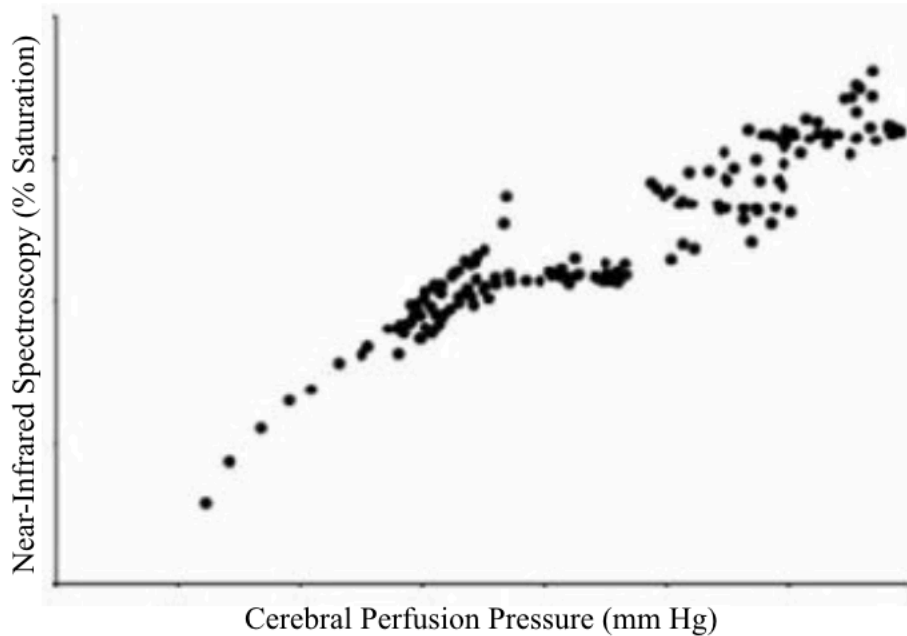
Figure 8: Scatter plot of near-infrared spectroscopy versus cerebral perfusion pressure in a pig [16].

Cerebral Autoregulation Monitoring in Humans

To extend this work into humans, the value of NIRS for time-domain autoregulation monitoring

was assessed in a study involving cardiac surgery patients [22]. In order to determine if NIRS

could serve as a replacement for TCD, this research team evaluated the strength of agreement

between TCD and NIRS-based methods [22]. COx error bar plots were generated using the

methods described above with ABP and NIRS as inputs [16, 22]. Error bar plots of the

correlation between ABP and TCD, which is known as the mean velocity index (Mx), were also

generated [22]. This data was averaged over the entire patient population to create one plot for

COx and one plot for Mx [22]. With this data, a statistically significant positive linear

relationship between COx and Mx was observed [22]. In addition, Bland-Altman analysis of Mx versus COx found low bias and good agreement [22].

Once validation studies of NIRS-based autoregulation monitoring had been performed in pigs and humans, several studies used this approach to determine whether ABP below the LLA was associated with morbidity after surgery that might be attributed to hypotension. In particular, Ono et al. sought to evaluate the association with AKI [1]. The first step in this analysis was to compute COx error bar plots for each patient using the methods described above. Then, the LLA from each plot was defined as the highest ABP at which the mean COx is greater than 0.3 [1]. Quantification of ABP below the LLA accounted for both time (hr) and pressure magnitude (mm Hg) spent below the LLA, and was calculated by subtracting the LLA from the ABP signal, computing the absolute value of the Riemann sum of the negative portion of this new signal to obtain the area of the ABP curve below the LLA (AUC), then applying time conversion factors and normalizing for time of cardiopulmonary bypass (CPB) to obtain an AUC per hour of CPB (mm Hg x min/hr) for each patient [1]. Patients who met at least the Risk criteria of RIFLE were classified as having AKI, while the rest were classified as having no AKI [1]. The distribution of AUC per hour of CPB was plotted in the no AKI and AKI groups, and the AKI group was found to have higher 25th percentile, median, and 75th percentile values of this measure of ABP below the LLA [1]. An ANOVA test rejected the null hypothesis that the no AKI and AKI groups have the same mean value of AUC per hour of CPB [1]. Similar findings have been demonstrated using other outcomes, with AUC also associated with major morbidity and mortality after cardiac surgery [27].

Limitations

Unfortunately, there are several limitations to this body of research. First, the clinical standards of surgery and anesthesiology have evolved over time [28]. For example, there have been notable changes in the types of cardiac procedures performed, such as a decrease in the number of aortic valve replacements due to the emergence of alternative procedures [29]. In addition, the criteria for diagnosing AKI have been updated from RIFLE to KDIGO [9]. For these reasons, it is uncertain if the original finding of an association between ABP below the LLA and AKI is generalizable to more recent practices.

In addition to changes in surgical and diagnostic practices, the methods for autoregulation monitoring used in prior studies also suggest a need for additional work. The LLA for each patient was chosen by clinician assessment of COx error bar plots, a process that limits the scalability of autoregulation research. The assumption that AUC would correspond more strongly with AKI than time below LLA needs to be evaluated. It is uncertain if the COx threshold of 0.3 used in prior studies is optimal for finding associations between AUC and AKI. In addition, it is unclear how baseline kidney function may affect the ability to tolerate renal insults.

1.3. Research Overview

The goals of this thesis are to address limitations of previous autoregulation research with the following aims: (1) to develop an algorithm that provides accurate, automated prediction of the LLA from COx error bar plots, (2) to determine if this algorithm can reproduce prior findings in a new study of AKI patients, and (3) to evaluate assumptions from prior research in order to discover the strongest associations between ABP below the LLA and AKI.

The first step in this process was to develop an algorithm for autoregulation analysis. For each patient, this algorithm identifies an LLA using error bar plots of COx versus ABP. The primary LLA selection method for this algorithm was designed to reproduce expert clinicians' LLA selection methods for a variety of threshold crossing patterns in COx error bar plots. The algorithm includes a secondary method that uses a parabola fit to mean COx values in an attempt to provide an LLA to plots that do not have a threshold crossing but do have a parabolic trend. The development of this algorithm, as well as evaluations of both the primary and secondary methods of LLA selection against an expert clinician's selections, are discussed in Chapter 2.

This algorithm was then utilized on data from a recent cohort of cardiac surgery patients to determine if the previous finding of a statistically significant association between AKI and AUC at a COx threshold of 0.3 is generalizable to new surgical practices, a new definition of AKI, and the methods used in the algorithm [1]. These results are shown in Chapter 3.

Finally, the assumptions of previous methods to characterize autoregulation were thoroughly evaluated. In particular, analysis was performed to assess how the association changes when time below LLA is the measure of ABP below the LLA (instead of AUC) or when the COx threshold for defining autoregulation failure is set to a value other than 0.3. In addition, subpopulations of patients with similar baseline kidney function were examined to see if stratification may reveal stronger associations between AUC and AKI. The findings from these sensitivity analyses are detailed in chapter 4.

Through this work, we aim to establish a new, efficient method for examining associations between AKI and ABP below the LLA. We summarize the findings obtained with this method in an attempt to provide information about how the utility of NIRS-based

autoregulation monitoring may be maximized in order to aid efforts to prevent perioperative

AKI.

Chapter 2

Developing and Testing an Algorithm for Automated LLA Selection

2.1. Introduction

A key challenge in applying autoregulation monitoring to clinical environments is the scalability of methods to estimate the lower limit of autoregulation (LLA). The current approach is based on expert assessment of graphs that depict the index of autoregulation versus ABP with a bin width of 5 mm Hg. Expert clinicians identify bins in which the mean index is above a specified threshold (e.g. COx = 0.3) as indicative of autoregulation failure, while bins in which the mean index is below the threshold are considered to represent intact autoregulation.

Unfortunately, there are shortcomings to current approaches. In prior autoregulation research, an expert clinician looked at each error bar plot and determined where the mean COx crossed below 0.3 in order to select an LLA for all patients. This method is not conducive to significant increases in cohort size for autoregulation research. Furthermore, there are many COx error bar plots in which the mean COx values do not cross the threshold line at all. This issue

limits the applicability of autoregulation monitoring methods in a large number of cardiac surgery patients.

The MATLAB algorithm presented in this thesis attempts to address some of these issues. This algorithm was developed with the goal of reproducing the LLA selections of expert clinicians by using mathematical rules. With the implementation of this algorithm, statistical tests for autoregulation research can be run on data from over 1000 patients within minutes. This algorithm scans the error bar plot from left to right and assigns the LLA by finding the first crossing of mean COx from above to below the threshold line. All plots without such a crossing, including upward sloping plots that may cross from below to above the threshold line, do not give an LLA. In order to provide an estimate for the LLA in some plots that do not have an LLA by threshold crossing, the algorithm also incorporates curve-fitting methods. Several studies have used a parabola with a positive quadratic coefficient to estimate the optimal cerebral perfusion pressure in error bar plots of autoregulation indices derived from intracranial pressure, and work by Zeiler et al. demonstrated the ability to do the same in plots with indices derived from transcranial Doppler [30, 31, 32]. Drawing inspiration from this prior work, our algorithm selects COx error bar plots that meet certain criteria as candidates for extrapolation of an LLA with a parabolic fit.

Before the algorithm can actually be used in autoregulation studies, it is important to establish that its methods for selecting an LLA are sufficiently accurate. Ideally, these evaluations would be performed in a way that accounts for the purpose of each LLA selection method: the threshold crossing method will substitute for expert selection of LLA values, while the parabola fit method can provide an LLA for select plots that do not have a threshold crossing.

This chapter discusses the development of the algorithm and the methods used to assess its accuracy compared with a gold standard of expert clinician rating.

2.2. Methods

2.2.1. Algorithm Development

For each patient, ABP and NIRS signals are used as inputs for the algorithm. These input signals have already been low-pass filtered with a moving average filter that computes the mean value in non-overlapping 10 second time windows. This filtering is performed with ICM+ software. The first step performed by the algorithm is to remove artifacts from filtered ABP and NIRS signals. This is done by removing values below the 6th percentile in ABP signals with a minimum value below 50 mm Hg and removing values above the 99.5th percentile in ABP signals with a maximum value above 150 mm Hg. A critical component in tuning this artifact correction method is ensuring removal of downward spiking artifacts, as these cause erroneously large values of area of the ABP curve below the LLA. With the filtered, artifact-corrected signals, the algorithm computes a continuous, moving Pearson's correlation coefficient between ABP and NIRS in overlapping 300 second (30 point) windows. This correlation data is referred to as the cerebral oximetry index (COx) [16]. Consecutive windows for correlation coefficient calculation overlap by 29 points. The algorithm then sorts each correlation coefficient value into an ABP bin of 5 mm Hg width according to the mean ABP in its 300 second window. The result is a COx error bar plot, which displays the mean COx as a point and the standard deviation of COx as error bars in each 5 mm Hg bin. If the number of COx data points in a bin constitutes less than 4% of the total number of COx data points, an error bar is not generated for this bin.

Data from 45 randomly selected patients were used in the development of this algorithm. Since each patient contributed both left and right-sided NIRS data, there were a total of 90 available COx error bar plots. Each plot had a threshold line at a COx value of 0.3. These plots were examined by expert clinicians, who determined the following: (1) presence or absence of an LLA, (2) an estimate of the LLA, and (3) if the error bar plot had a u-shape. The latter is important to identify promising candidates for LLA extrapolation with a parabolic fit.

The first step performed by the algorithm is to identify the LLA based on the ABP value at which the mean COx crosses below a user-specified threshold. The following rules were incorporated into the algorithm:

- When scanning the plot from left to right, identify the first point in which one ABP bin has a mean COx above the threshold line and the ABP bin directly to its right has a mean COx below the threshold line. If there is no such crossing, the plot does not have an LLA. If there is such a crossing, the LLA is defined as the upper ABP limit of the bin on the right side of this crossing, unless the only such crossing occurs at the far right end of the error bar plot.

Figure 9 includes examples of error bar plots that illustrate these threshold crossing rules.
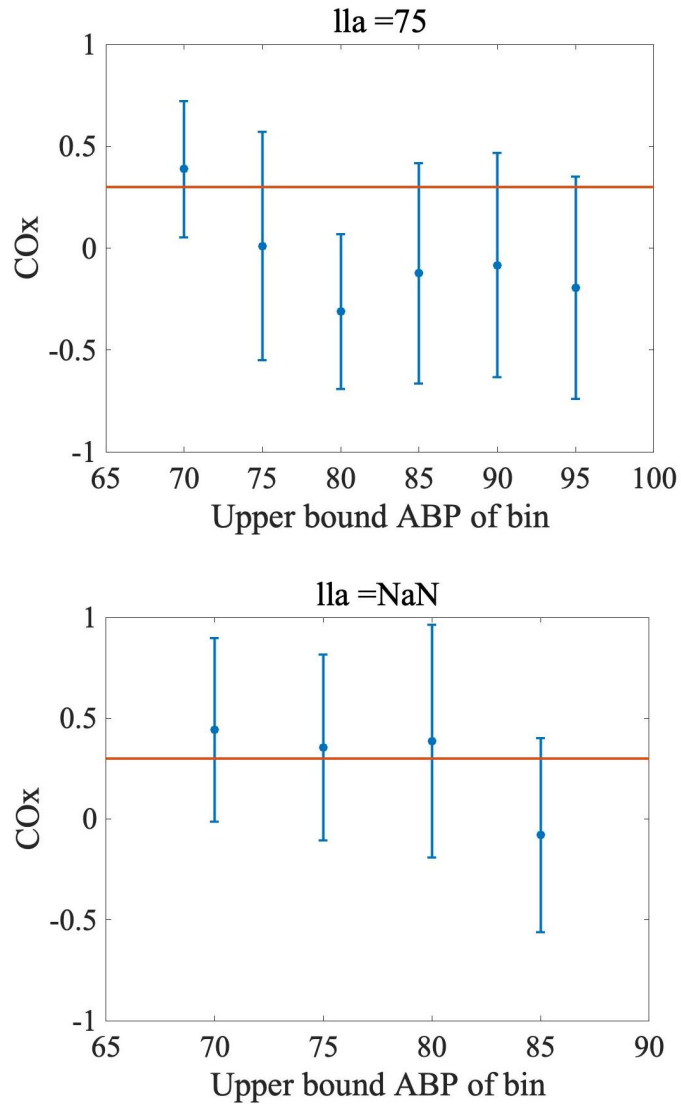
Figure 9: Examples of LLA selection by threshold crossing. LLA values are shown above each plot, where NaN indicates absence of an LLA. The bottom plot does not have an LLA because the crossing from above to below the threshold occurs at the far right end of the plot.

The second step performed by the algorithm is to identify u-shaped curves via the following rules:

1. The best fit parabola to the mean COx values has a positive quadratic coefficient.

2. There are error bars on both sides of the minimum value of the parabola. This step ensures that both the increasing and decreasing parts of the parabola fit to data.

3. The norm of the residuals of the parabola fit is less than 0.4. This maximum acceptable error of parabola fit was found to enable all expert selected u-shaped plots to be classified as such while reducing the false positive rate observed when implementing only the first two criteria.

The final step performed by the algorithm is to identify the LLA with a parabola fit to the mean COx values for plots that meet the following criteria:

1. The plot has been classified as u-shaped.

2. The plot shape does not indicate the potential for multiple crossings around the threshold line. As shown in Figure 10, plots with this shape characteristic can have an uncertain LLA based on threshold crossing. Therefore, they are not suitable for LLA extrapolation through a parabola fit because even expert selection is unreliable.
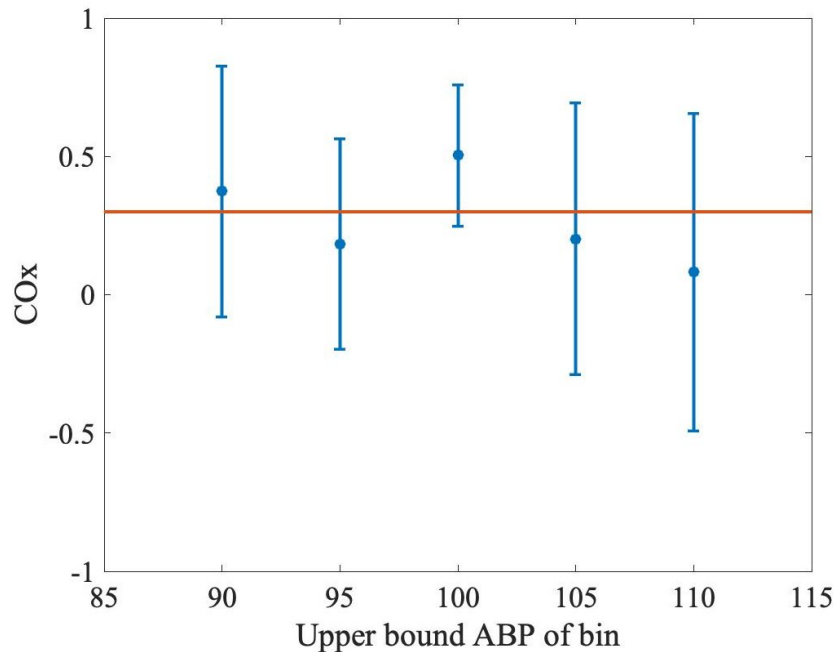
Figure 10: Example of plot with uncertain LLA based on threshold crossing.

For plots that meet all four criteria for parabola fit LLA selection, the LLA is chosen as the ABP value at which the decreasing portion of the parabola intersects the threshold line. To make the precision consistent with LLA selection by threshold crossing, the ABP value at the intersection is rounded up to the nearest multiple of 5 to give the final parabola fit LLA. The parabola fit LLA is discarded if it is estimated to be less than 50, greater than 100, or more than 10 mm Hg from the closest error bar.

The algorithm was developed in an iterative process with clinician input and application to the 90 aforementioned error bar plots. For each iteration of the algorithm, expert clinicians identified incorrect LLA selections, as well as false positives and false negatives in u-shape classification. With these cases in mind, the algorithm was adjusted to generate new LLA selection and u-shape classification results. These adjustments included updates to the LLA assignment rules for certain threshold crossing patterns or a change in the maximum allowable norm of residuals of the parabola fit. This process was repeated until the algorithm's LLA selections and u-shape classification results both achieved accuracy of over 80%.

2.2.2. Evaluation of Algorithmic LLA Selection Methods

In order to validate the newly-developed algorithm against a gold standard of expert clinician rating, a series of 50 patients contributing 100 error bar plots were selected. The plots of these patients were not used in algorithm development. Each plot had a threshold line at a COx value of 0.3. The algorithm was used to identify LLA values with both the threshold crossing method and the parabola fit method. Separately, an expert clinician identified LLA values based on

threshold crossing patterns in the same error bar plots. The latter estimates were treated as the ground truth for comparison.

The first comparison of interest was agreement in identification of presence or absence of an LLA. For patients with LLA estimates, several approaches were used to compare algorithmic LLA selections to those of the expert clinician. First, scatter plots were generated to visualize the data. Second, a root mean square error (RMSE) of LLA prediction by the algorithm compared to expert selections was computed. Finally, a Bland-Altman plot was generated to find the 95% confidence interval for the difference between LLA selections by the algorithm and by the expert clinician [33].

2.3. Results

2.3.1. Algorithm LLA by Threshold Crossing

Expert rating indicated that 33% (33/100) of the plots had an LLA, and the remaining 67% (67/100) did not. The reasons for absence of LLA estimates in 67 plots are shown in Table 1.

Reason for absence of LLA	Number of plots
Upward sloping	16
All mean COx values below threshold	32
All mean COx values above threshold	10
Threshold crossing at far right end	7
LLA outside expected ABP range	1
One error bar	1

Table 1: Reasons for absence of LLA estimate.

The algorithm's threshold crossing method resulted in 34 plots with an LLA and 66 plots without one. When considering the plots that the expert clinician assigned an LLA as belonging to the positive class, the algorithm gave a sensitivity of 100% and a specificity of 98.5%.

There were 33 error bar plots with LLA estimates from the algorithm by threshold crossing and from expert rating. The scatterplot of these estimates is shown in Figure 11. For 32 of these instances, the expert and algorithm LLA selections were the same, giving an accuracy of 97.0% and an RMSE of 0.870 mm Hg. In one case, the algorithm overestimated the LLA by 5 mm Hg.
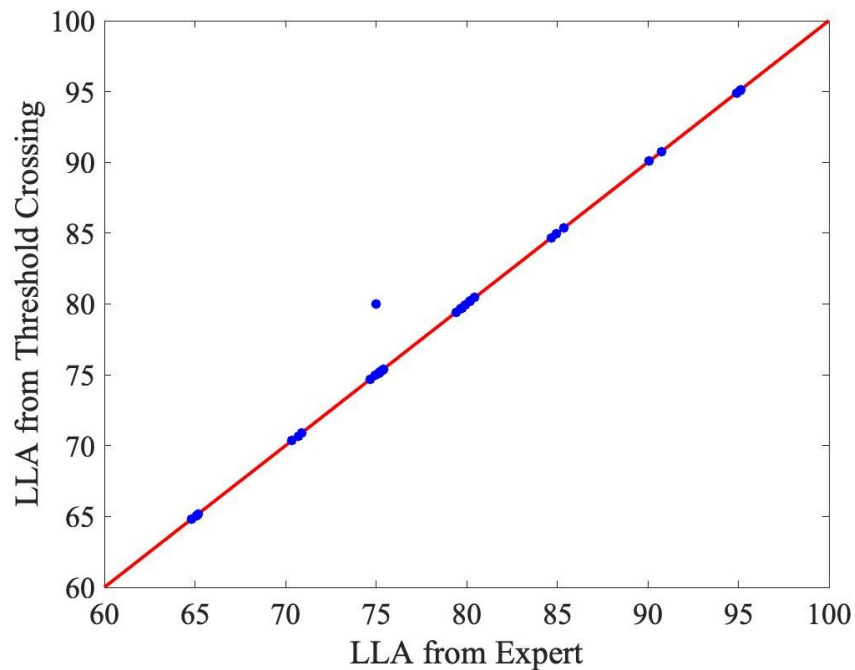
Figure 11: Scatter plot of algorithm LLA by threshold crossing versus expert LLA. The line y = x is displayed as an indicator of correct prediction. Noise was added to each x-y pair to reduce overlap for visualization purposes only.

The Bland-Altman plot for these 33 estimates is shown in Figure 12. The mean of algorithm LLA minus expert LLA was 0.152 mm Hg, and the standard deviation of this difference was 0.870 mm Hg. This gave a 95% confidence interval for the difference that had a lower bound of -1.554 mm Hg and an upper bound of 1.857 mm Hg. Overall, when taking into account true negatives and true positives with the exact same LLA value, the algorithm's selection matched with the expert's selection for 98 out of 100 plots.
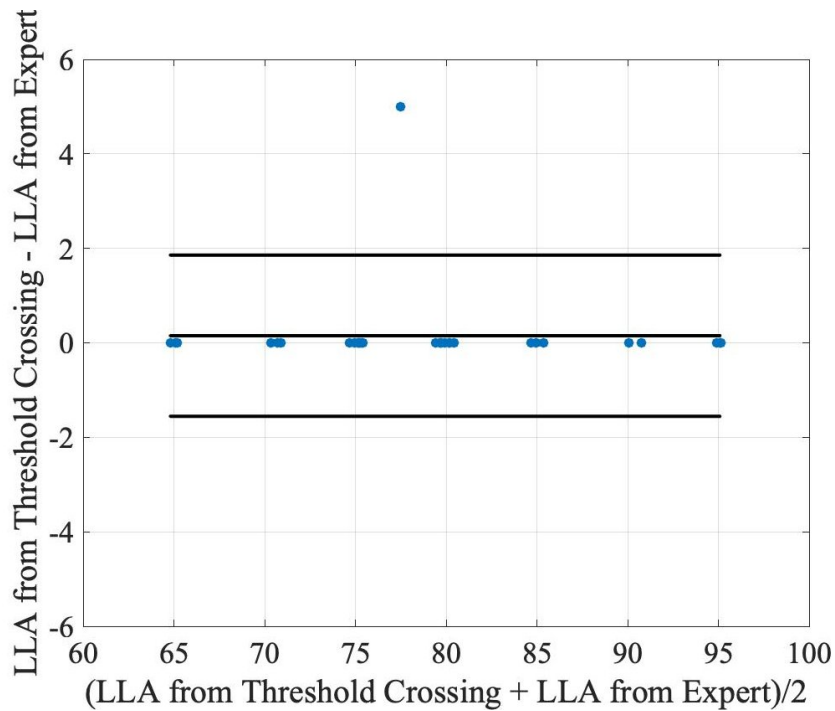
Figure 12: Bland-Altman plot comparing algorithm LLA selections by threshold crossing to expert selections. The lines display the mean and 95 percent confidence interval boundaries for the difference between these selections. Noise was added to each x-y pair to reduce overlap for visualization purposes only.

2.3.2. Algorithm LLA by Parabola Fit

The parabola fit method computed an LLA for 35 out of the 100 error bar plots. Since only 15 of

these plots had an LLA by expert selection, these were the only ones that could be used for

comparison. A scatter plot of LLA estimates by parabola fit and by expert clinician is shown in

Figure 13. For 13 of these 15 plots, the expert and parabola fit LLA selections were the same,

giving an accuracy of 86.7% and an RMSE of 1.826 mm Hg. The parabola fit overestimated the

LLA by 5 mm Hg in one case and underestimated it by 5 mm Hg in another case.
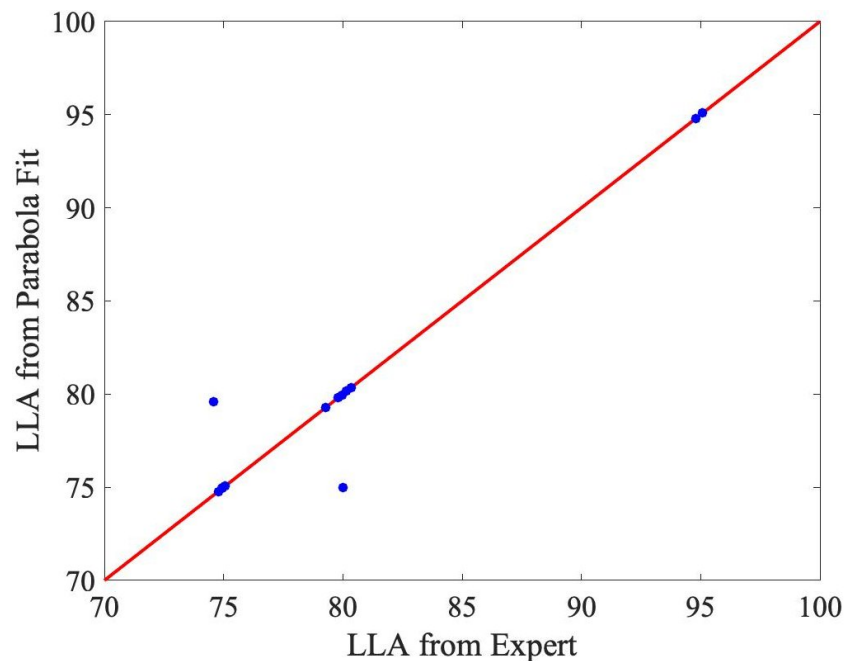
Figure 13: Scatter plot of algorithm LLA by parabola fit versus expert LLA. The line y = x

is displayed as an indicator of correct prediction. Noise was added to each x-y pair to

reduce overlap for visualization purposes only.

The Bland-Altman plot for these 15 estimates is shown in Figure 14. The mean of parabola fit LLA minus true LLA was 0 mm Hg, and the standard deviation of this difference was 1.890 mm Hg. This gave a 95% confidence interval for the difference that had a lower bound of -3.704 mm Hg and an upper bound of 3.704 mm Hg.
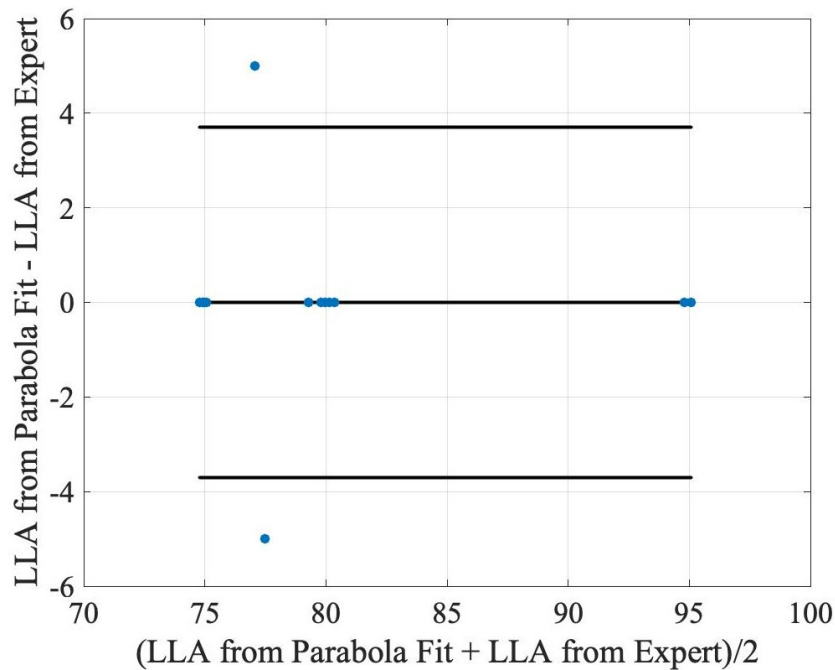
Figure 14: Bland-Altman plot comparing algorithm LLA selections by parabola fit to expert selections. The lines display the mean and 95 percent confidence interval boundaries for the difference between these selections. Noise was added to each x-y pair to reduce overlap for visualization purposes only.

2.4. Conclusions

In this chapter, we discussed an algorithm that we developed to analyze COx error bar plots and evaluated its accuracy in LLA selection on data from 50 patients. The algorithm's threshold crossing method for LLA selection was highly accurate when compared to expert assessment. The parabola fit method for LLA selection showed strong performance in increasing the number of patients with an LLA and showed high agreement with expert selections in plots with a threshold crossing.

The first method in the algorithm, LLA selection by threshold crossing, was designed to reproduce the gold standard method performed by trained experts who analyze error bar plots. This method of LLA selection is the most critical in ensuring that the algorithm serves its purpose of producing accurate autoregulation research results in a timely manner with large patient sets. With this method, the algorithm selection agreed with the expert clinician selection in 98 out of 100 plots, and in 32 out of 33 plots for which both methods gave a numerical value for the LLA. The algorithm was only off by one bin in the case for which both methods gave an LLA but they disagreed. It is notable that in the Bland Altman plot, the lower and upper bounds of the 95% confidence interval both had a magnitude smaller than the 5 mm Hg distance between consecutive bins. While these results show high accuracy, they also show that the threshold crossing method is not 100% accurate even though it was developed in an iterative process. This may be partially explained by the fact that the true LLA values are not certain, and the expert clinician's selections may not be 100% accurate either. Nonetheless, we determined the threshold crossing method to be sufficiently accurate for use in analyses involving measures of AKI outcomes.

The second method, LLA selection by parabola fit, was intended to provide an estimate of the LLA for select plots that do not have a threshold crossing. The parabola fit LLA method selected 35 out of the 100 plots for LLA extrapolation. Out of these plots, 20 did not have an LLA by threshold crossing. If the parabola fit method were to be used in this algorithm, it would be used at the same time as the threshold crossing method in order to increase sample size of analyses. Given that it assigned an LLA to nearly 30% of plots without a threshold crossing, it appeared to be a valuable tool for this purpose. Unfortunately, since the only gold standard available for LLA selection with ABP and NIRS is expert selection by threshold crossing in COx error bar plots, the assessment of parabola fit LLA selection relied on plots for which this approach would likely not be used in autoregulation research. Although this evaluation was not a true validation, it was an informative exercise about the strength of selection criteria for the parabola fit method. Among the 15 plots that had a numerical value of the LLA by parabola fit and by expert clinician, these selections agreed in 13 plots. While these results do suggest that the parabola fit method is a useful tool for increasing sample size and has reasonable selection criteria, there is still uncertainty about its accuracy in plots that do not have a threshold crossing. Due to this concern, as well as the desire to closely follow the LLA selection methods of Ono et al., the parabola fit method is not used in the following chapters [1]. However, the appendices show the association between ABP below the LLA and AKI when using both methods of algorithmic LLA selection.

A major limitation was the inability to select an LLA in a significant number of plots. Over 40% of plots did not have an LLA by threshold crossing or parabola fit. Future work should

incorporate other curve fitting methods in order to maximize generalizability of autoregulation

research results.

Chapter 3

Demonstrating an Association of AUC with Acute Kidney Injury in a New Cohort of Cardiac Surgery Patients

3.1. Introduction

Prior research has suggested an association between the area of the ABP curve below the LLA (AUC) and the development of acute kidney injury (AKI) in patients undergoing cardiac surgery [1]. This finding is significant because it implies that targeting blood pressure above the cerebral LLA during surgery may be an effective method of reducing the occurrence of perioperative AKI.

However, there are several concerns that suggest that this finding needs additional validation. Most obvious among these is the lack of other studies which have investigated and replicated these findings. In addition, there have been significant changes in cardiac surgery practices. The methods of surgeons and anesthesiologists have been altered, there has been a

substantial reduction in the number of aortic valve replacement surgeries, and new anesthetic medications have been introduced [28, 29, 34, 35]. Furthermore, this research relied on LLA selection by expert clinician assessment of COx error bar plots, a process which has poor scalability.

The work in this chapter attempted to reproduce the findings by Ono et al. with a more recent cohort of patients and updated methods [1]. We kept much of the same methodology, including the use of AUC to measure ABP below the LLA. However, there were two key differences. First, we utilized the algorithm discussed in Chapter 2 in order to automate LLA selection. Second, our work used the KDIGO criteria to define AKI because this is the most recent method [9]. Reproducing prior results with these altered methods would be a strong indication that the finding of an association between AUC and AKI is generalizable to new surgical practices and definitions of AKI, and would imply that an algorithmic approach is suitable for finding these associations.

3.2. Methods

3.2.1. Patient Population

Two cohorts of patients were used for this analysis. Patients in the first cohort (n=173) were enrolled between 2016-2018, and enrollment criteria were undergoing cardiopulmonary bypass, with planned coronary artery bypass graft surgery (CABG) and/or valve surgery and/or aortic surgery and/or myectomy. Exclusion criteria were planned heart or lung transplant or left

ventricular assist device. Patients in the second cohort (n=172) were enrolled in 2018-2019 and the primary enrollment criterion was undergoing cardiopulmonary bypass.

3.2.2. Calculation of AUC

For each patient, the algorithm was used to generate left and right COx error bar plots and estimate the LLA from each of these plots based on the threshold crossing method, as described in Chapter 2. The COx threshold was set to 0.3, since this was the value used by Ono et al. [1]. Given that the two COx error bar plots for a patient did not always give the same value for the LLA, rules were developed to select one LLA for each patient. These rules are:

1. If both plots give a numerical value of the LLA, the patient's LLA is the greater of the two values.

2. If only one plot gives a numerical value of the LLA, then it is automatically selected for the patient.

3. If both plots give no LLA, the patient is considered not to have an LLA.

With the selected LLA value, AUC was calculated by subtracting the LLA from the ABP signal, computing the absolute value of the Riemann sum of the part of this new signal that lies below 0, then dividing by a conversion factor to give units of mm Hg x hr. Outliers were removed by excluding patients with AUC values above the 95th percentile from all analyses because of concerns that a few plots with inaccurate LLA selections could introduce substantial error in results.

37

3.2.3. Definition of AKI

AKI was identified according to the KDIGO criteria using baseline and post-operation serum creatinine (SCr) levels in mg/dL. According to this method, all patients who experienced an increase in SCr of at least 0.3 mg/dL within 48 hours of surgery or an increase in SCr above baseline by a factor of at least 1.5 within 7 days of surgery met the minimum criteria for Stage 1 AKI, and were therefore labeled as AKI patients [36]. The remaining patients were labeled as having no AKI.

3.2.4. Analytic Plan

Exploratory data analysis was conducted to examine the quality of the data and to visualize the data using charts and tables. A Wilcoxon rank-sum test was performed to assess the statistical significance of the difference in median value of AUC between patients who were classified as not having AKI and those who were classified as having AKI. This was a one-tailed test with the alternative hypothesis that the median AUC of the no AKI group is less than the median AUC of the AKI group. Box plots of AUC for the no AKI and AKI groups were created to display the median and interquartile range of AUC for each group. A logistic regression model was generated with AUC as the predictor variable and KDIGO definition of AKI as the outcome variable. The odds ratio was computed as e^{β_1}, where β_1 represents the coefficient for the predictor variable AUC in the log odds equation obtained from logistic regression [37]. The Wald confidence interval for β_1 was used to generate the 95% confidence interval for the odds ratio [38]. These odds ratio results were exponentiated by a factor of 10, so that the odds ratio and 95% confidence interval reported gave the factor by which the odds of AKI increased per 10 mm

Hg x hr increase in AUC [39]. In addition, the p-value of AUC in the logistic regression model was reported.

3.3. Results

3.3.1. Patient Population

The characteristics of the 345 patients whose data was used in this analysis are shown in Table 2. The incidence of AKI was 20.6% (71/345). The estimated glomerular filtration rate (eGFR) for each patient was calculated using the Modification of Diet in Renal Disease (MDRD) equation, which is a function of baseline serum creatinine concentration, age, race, and sex [40]. The mean baseline eGFR for this population was 75.5 mL/min/1.73 m^2, which falls into the category of mildly reduced kidney function [41]. However, there was substantial variation in baseline kidney function among these patients, with a standard deviation of 28.1 mL/min/1.73 m^2.

Patient Characteristics		
Age	(mean $\pm$ SD)	62.5 $\pm$ 12.2
Sex	Female, n (%)	93 (27.0%)
	Male, n(%)	252 (73.0%)
AKI	No AKI, n (%)	274 (79.4%)
	AKI, n (%)	71 (20.6%)
Baseline eGFR (mean $\pm$ SD)		75.5 $\pm$ 28.1

Table 2: Characteristics of the 345 patients analyzed. (AKI = acute kidney injury, eGFR = estimated glomerular filtration rate)

3.3.2. Comparison of AUC According to Development of AKI

An LLA was available for 162 patients for use in this analysis. Out of these patients, the incidence of AKI was 25.3% (41/162). The group of patients who did not have AKI had a mean LLA of 79.0 mm Hg and a mean baseline SCr of 1.2 mg/dL, while the group of patients who had AKI had a mean LLA of 76.5 mm Hg and a mean baseline SCr of 1.4 mg/dL. The combined distribution of AUC values for these 162 patients was skewed, with a median of 25.8 mm Hg x hr (IQR 17.0, 37.9). The histograms of AUC for the no AKI and AKI groups are shown in Figure 15.
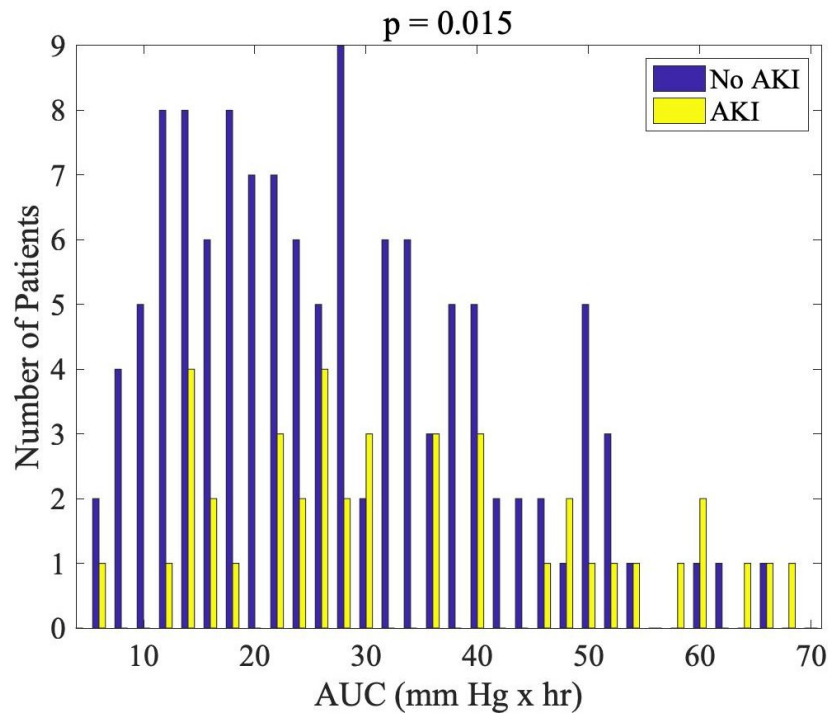
Figure 15: Histograms of AUC for no AKI and AKI groups. The p-value of the rank-sum test is shown above.
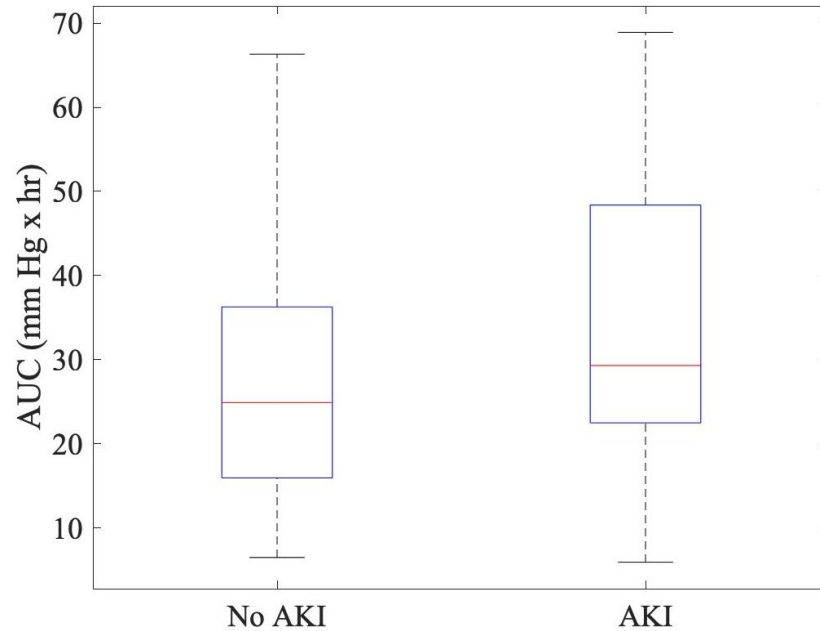
Figure 16: Box plots of AUC for no AKI and AKI groups.

Figure 16 shows the box plot distribution of AUC by AKI status.The median, 25th percentile, and 75th percentile values of AUC were all higher in patients with AKI, who had a median of 29.3 mm Hg x hr (IQR 22.5, 48.4) compared with patients without AKI, who had a median of 24.9 mm Hg x hr (IQR 15.9, 36.3). The rank-sum test returned a p-value of 0.015.

The logistic regression model returned an odds ratio of 1.35 per 10 mm Hg x hr increase in AUC, with a 95% confidence interval of 1.07-1.71 and a p-value of 0.013. This odds ratio represents an increase in odds of AKI by a factor of 6.66 as AUC increases from the minimum value to the maximum value in this patient population.

3.4. Conclusions

In this chapter, we found a statistically significant association between AUC and AKI, which is consistent with prior research in this field [1]. Specifically, the median value of AUC was higher for a population with AKI than for a population without AKI. The p-value of AUC from logistic regression implies that it was statistically significant as a predictor of AKI. This ability to produce similar findings to prior work suggests that the association between AUC and AKI is generalizable to updated surgical practices and a change from RIFLE to KDIGO criteria. It is also notable that the change from expert clinician selection of LLA values to algorithmic LLA selection by threshold crossing did not affect the ability to find this association. The implication of this is that the algorithm may be a viable option for efficient LLA selection in large patient sets.

There are multiple limitations to this work that merit discussion. The most important one is that roughly 53% of patients in the study were excluded from this analysis. The majority of these patients did not have an LLA by threshold crossing, and a few were excluded because they had AUC values above the 95th percentile. This issue prevents the use of COx-based autoregulation monitoring for all cardiac surgery patients, and limits widespread applicability of these methods. The fact that the distributions of AUC values for the AKI and no AKI groups displayed nearly complete overlap is another major concern. Despite the statistical significance of the rank-sum test result, this overlap means that the overwhelming majority of cardiac surgery patients could not be confidently diagnosed as having or not having AKI based on their AUC value alone, and thus it would be difficult to generate prediction models using this data. This interpretation is supported by the low odds ratio relative to the range of AUC values. Due to

these limitations, it appears that exploring the ability to find stronger associations between ABP

below the LLA and AKI is a worthwhile endeavor. Chapter 4 discusses work done with this goal

in mind.

Chapter 4

Sensitivity Analyses

4.1. Introduction

The results of Chapter 3 demonstrated a statistically significant association between AUC (mm Hg x hr) and AKI defined by KDIGO criteria when LLA is defined using a COx threshold of 0.3. These results confirm prior findings by Ono et al. [1]. However, this prior research relied on several assumptions, including that AUC would be the measure of ABP below the LLA most closely associated with AKI and that a COx threshold of 0.3 is most appropriate for defining the LLA [1]. In order to find the strongest association between ABP below the LLA and AKI, it is important to test these assumptions. Additionally, given differential vulnerability of patients to AKI according to baseline kidney function, we aimed to examine whether the association between AUC and AKI would be differential by baseline kidney function. Each of these issues is discussed in more detail below.

4.1.1. Use of Time Below LLA

Prior research involving autoregulation and AKI, as well as the results in Chapter 3, quantified ABP below the LLA based on AUC [1]. However, there is reason to believe that time-based measures of ABP below the LLA may be valuable as well. Using recordings from traumatic brain injury patients in the intensive care unit, researchers generated logistic regression models in

which variables based on time below the optimal cerebral perfusion pressure were statistically significant predictors of survival 6 to 12 months later [42]. To evaluate if such strong associations can be found with AKI outcomes, this chapter analyzes association to AKI when time below LLA is used instead of AUC.

4.1.2. Varying the COx Threshold

Pig studies have found that a COx value above 0.36 corresponds with autoregulation failure defined by a gold standard method of LLA estimation [16]. However, it is unclear if these results would be generalizable to humans with hypertension, cerebrovascular disease, and other comorbidities. Although human studies have found a COx threshold of approximately 0.3 to match closely with thresholds derived from autoregulation measurements of the LLA using transcranial Doppler, there is no gold standard to identify the LLA in humans [22]. In order to examine different COx thresholds to identify the LLA, this chapter reports a systematic evaluation of COx threshold values both above and below 0.3. An ideal result would show strong associations between AUC and AKI at particular clusters of COx threshold values.

4.1.3. Stratification by Baseline eGFR

Baseline estimated glomerular filtration rate (eGFR) is an important variable to consider when looking for an association between AUC and AKI. AKI is defined by a significant decline in GFR that is often caused by a decrease in renal blood flow [43]. Therefore, patients who already have a low eGFR at baseline may be more vulnerable to the effects of renal hypoperfusion caused by ABP below the LLA [5, 9]. On the other hand, patients with a high eGFR at baseline

have normal kidney function and may not be as vulnerable. We hypothesized that AUC would be more important in terms of risk of AKI in patients with impaired kidney function at baseline than in patients with normal kidney function at baseline.

4.2. Methods

4.2.1. Patient Population

The patients in this chapter are the same patients examined in Chapter 3. Briefly, two cohorts of patients were used for this analysis, with 173 in the first cohort and 172 in the second cohort, for a combined total of 345 patients.

4.2.2. Calculation of Autoregulation Parameters

For analyses using time below LLA, LLA values were selected from error bar plots at a COx threshold of 0.3 by the threshold crossing method, as described in Chapter 2. Time below LLA was calculated by counting the number of indices in the 10 second averaged ABP vector that do not contain an ABP value above the LLA, then applying a time conversion factor so that this number represents time in hours. Outliers were removed by discarding time below LLA values above the 95th percentile.

For threshold value optimization, the COx threshold was varied between 0.1 and 0.5 with increments of 0.025, so that analysis was performed at 17 different COx threshold values. At each COx threshold value, the LLA was computed by the threshold crossing method discussed in

Chapter 2 and AUC was computed with the same method described in Chapter 3. Outliers were removed by discarding AUC values above the 95th percentile.

4.2.3. Calculation of Baseline Kidney Function

Patients were divided into subpopulations according to baseline eGFR. This baseline eGFR was computed with the Modification of Diet in Renal Disease (MDRD) equation [40]. One subpopulation contained all patients with eGFR below 60, which includes those with moderately and severely reduced kidney function as well as those with end-stage kidney failure [41]. The other subpopulation contained all patients with eGFR greater than 60, which represents mildly reduced or normal kidney function [41]. For eGFR stratified analysis, we then computed LLA values at a COx threshold of 0.3 using the threshold crossing method. AUC values were computed as described in Chapter 3. Outliers were removed by discarding AUC values above the 95th percentile.

4.2.4. Definition of AKI

AKI was identified according to the KDIGO criteria using baseline and post-operation serum creatinine (SCr) levels in mg/dL. According to this method, all patients who experienced an increase in SCr of at least 0.3 mg/dL within 48 hours of surgery or an increase in SCr above baseline by a factor of at least 1.5 within 7 days of surgery met the minimum criteria for Stage 1 AKI, and were therefore labeled as AKI patients [36]. The remaining patients were labeled as having no AKI.

4.2.5. Analytic Plan

Exploratory data analysis was conducted to examine the quality of the data and to visualize the data using charts and tables.

Similar steps were taken to examine the association between time below LLA and AKI and the association between AUC and AKI in subpopulations stratified by baseline kidney function. For each of these analyses, we generated data sets containing a measure of ABP below the LLA (AUC or time below LLA) and an AKI outcome label for each patient. A COx threshold of 0.3 was used to identify the LLA, and a one-tailed Wilcoxon rank-sum test was performed to test the alternative hypothesis that the AKI group has a higher median value of the measure of ABP below the LLA than the no AKI group. In addition, box plots of the measure of ABP below the LLA for the no AKI and AKI groups were made to display the median and interquartile range for each group. Logistic regression models were generated with the measure of ABP below the LLA as the predictor variable and KDIGO definition of AKI as the outcome variable. For each model, the p-value of the measure of ABP below the LLA was reported, and p-values less than 0.05 were considered significant. The odds ratio and its 95% confidence interval for AUC are reported as odds ratio per 10 mm Hg x hr increase in AUC. The odds ratio and its 95% confidence interval for time below LLA are reported as odds ratio per 1 hr increase in time below LLA.

The logistic regression model for AUC from Chapter 3 and the model for time below LLA from this chapter were used to generate logistic functions for probability of AKI. With these functions, the probability of AKI was computed for all 162 patients with an LLA. Using these probabilities, we generated receiver operating characteristic (ROC) curves and computed the area

under the ROC curve to compare time below LLA and AUC based on their ability to predict AKI.

When testing different COx thresholds, we generated logistic regression models with AUC calculated using the LLA identified at each COx threshold. At each threshold, the odds ratio per 10 mm Hg x hr increase in AUC is reported. Multiple comparison correction of p-values was performed with the Benjamini-Yekutieli procedure at 5% significance. This method assumes dependence between the logistic regression models but not necessarily positive correlation [44].

4.3. Results

4.3.1. Patient Population

There were 345 patients whose data was used for this analysis. The mean age was 62.5 years, with a standard deviation of 12.2 years. 73.0% of patients were male and 27.0% were female. According to the KDIGO criteria, 20.6% of patients had AKI. After eGFR values were calculated with the MDRD equation, 25.2% of patients were found to have an eGFR less than 60.

4.3.2. Use of Time Below LLA

There were 162 patients who had an LLA, and the incidence of AKI among these patients was 24.1% (39/162). For the no AKI group, the median value of time below LLA was 3.3 hr (IQR 2.7, 4.1). For the AKI group, the median value of time below LLA was 3.8 hr (IQR 3.2, 4.6). The p-value of the one-tailed rank-sum test was 0.0095. Figure 17 shows histograms for these time below LLA distributions with a bin size of 0.25 hr. Figure 18 contains box plots of the distribution of time below LLA values for the no AKI and AKI groups.
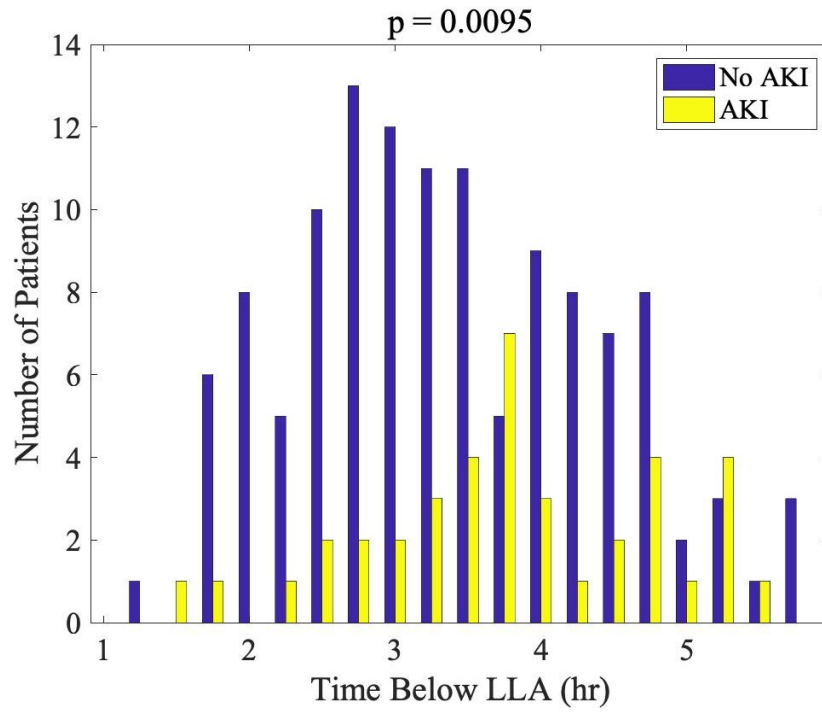
Figure 17: Histograms of time below LLA for no AKI and AKI groups. The p-value of the rank-sum test is shown above.
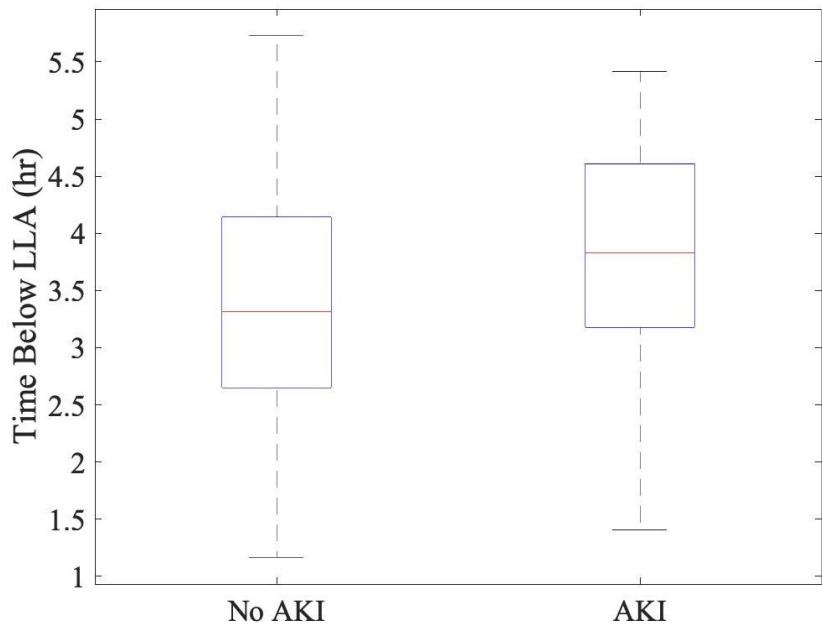
Figure 18: Box plots of time below LLA for no AKI and AKI groups.

The logistic regression model returned an odds ratio of 1.51 per 1 hr increase in time below LLA, with a 95% confidence interval of 1.05-2.17 and a p-value of 0.026. This odds ratio represents an increase in the odds of AKI by a factor of 6.56 as time below LLA increases from the minimum to the maximum value in this population.

The ROC curves for AUC and time below LLA at a COx threshold of 0.3 are shown in Figure 19. The area under the ROC curve for AUC was 0.614, and the area under the ROC curve for time below LLA was 0.625. For the model that generated probability of AKI as a function of time below LLA, the probability of AKI was less than 0.5 for all time below LLA values in this patient population. For the model that generated probability of AKI as a function of AUC, the probability of AKI was greater than 0.5 only for the highest AUC value in the patient population, and was less than 0.5 for the remaining 161 AUC values.

In these results, time below LLA and AUC at a COx threshold of 0.3 showed comparable strengths of association with AKI.
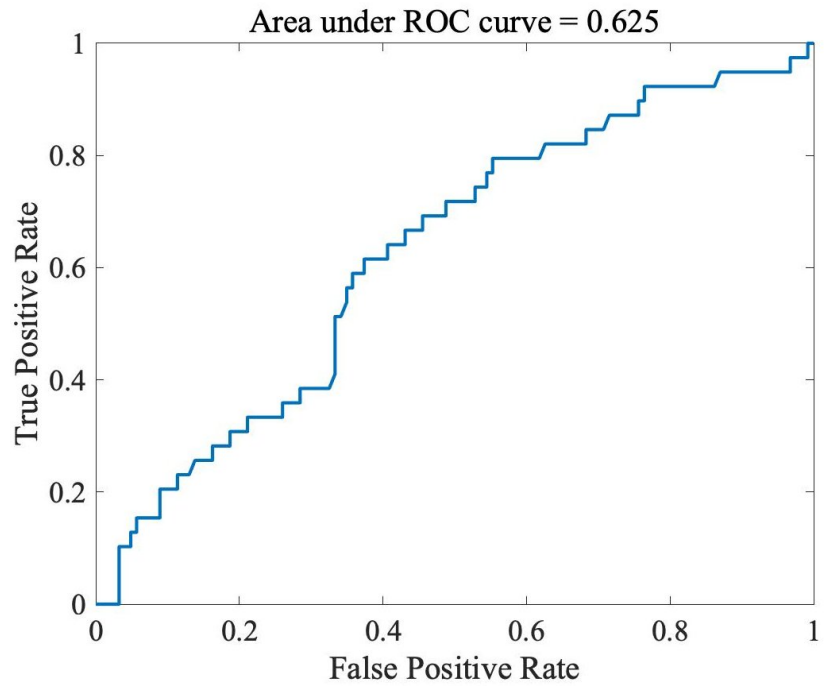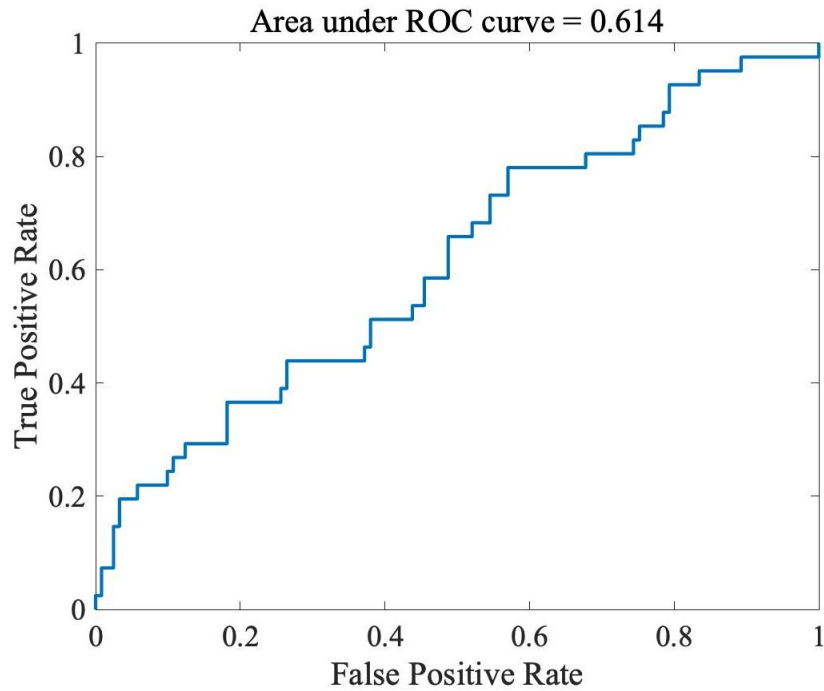
Figure 19: ROC curves at a COx threshold of 0.3. The top curve was generated with AUC as the predictor variable, and the bottom curve used time below LLA. The area under each ROC curve is shown above.

4.3.3. Varying the COx Threshold

Table 3 shows the outputs of logistic regression models that estimate the odds of AKI at each COx threshold, as well as the number of patients with an LLA (excluding outliers) at each threshold. These results reveal a cluster from COx thresholds 0.325 through 0.4 that contains four of the six highest odds ratios and four of the five lowest p-values among all of the COx thresholds used. A similar cluster occurs from COx thresholds 0.125 through 0.15. Only COx threshold values from 0.15 through 0.325 provided an LLA for more than 40% of the 345 patients in this population. Among these eight threshold values, 0.15 and 0.325 had the highest odds ratios, with each giving an odds ratio of approximately 1.45 per 10 mm Hg x hr increase in AUC. The lowest p-value among these eight threshold values was 1.63×10^{-3} at a COx threshold of 0.325. Figure 20 shows the plot for multiple comparison correction of p-values at 5% significance. The seven lowest p-values were below the correction line, and therefore remained statistically significant after multiple comparison correction [44]. These p-values occurred at COx thresholds of 0.125, 0.15, 0.275, and 0.325 through 0.4.

While this analysis contained two clusters of COx thresholds that have a strong association between AUC and AKI, the cluster from 0.325 through 0.4 was consistent with findings of prior autoregulation research in both pigs and humans [16, 22]. Furthermore, a COx threshold of 0.325 provided the maximum number of patients with an LLA out of all threshold values in these two clusters of strong association.

COx threshold	Odds ratio (OR)	95% CI	p-value	Number of patients with an LLA
0.1	1.36	1.02-1.80	0.037	114
0.125	1.47	1.12-1.94	5.75×10^{-3}	129
0.15	1.45	1.14-1.85	2.50×10^{-3}	142
0.175	1.27	1.02-1.58	0.029	146
0.2	1.28	1.01-1.62	0.039	149
0.225	1.19	0.97-1.47	0.096	159
0.25	1.29	1.02-1.62	0.032	162
0.275	1.43	1.13-1.81	2.76×10^{-3}	159
0.3	1.35	1.07–1.71	0.013	162
0.325	**1.45**	**1.15–1.83**	**1.63×10^{-3}**	**157**
0.35	**1.45**	**1.14–1.86**	**2.69×10^{-3}**	**135**
0.375	**1.59**	**1.24–2.05**	**3.22×10^{-4}**	**137**
0.4	**1.63**	**1.23–2.17**	**6.66×10^{-4}**	**127**
0.425	1.41	1.08–1.86	0.013	123
0.45	1.34	1.00–1.79	0.046	112
0.475	1.24	0.89–1.72	0.202	102
0.5	1.09	0.76–1.57	0.644	87

Table 3: Statistics for logistic regression with AUC as predictor of AKI at 17 different COx threshold values. Statistics reported include odds ratio per 10 mm Hg x hr increase in AUC and its 95 percent confidence interval, p-value of AUC in logistic regression, and number of patients with an LLA.
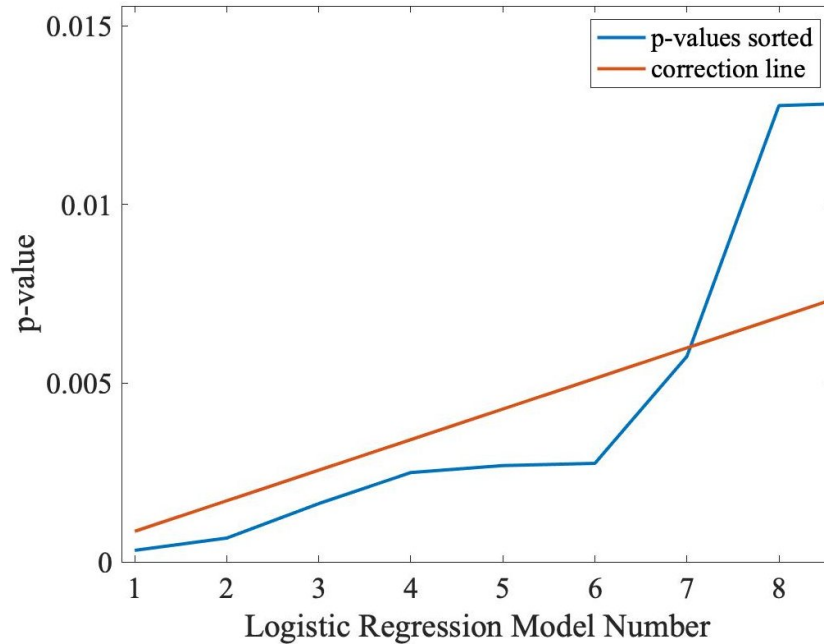
Figure 20: Multiple comparison correction of p-values from logistic regression by the Benjamini-Yekutieli procedure at 5 percent significance. Logistic regression models are sorted in order of increasing p-value, and the plot is zoomed in on the eight lowest p-values. The seven lowest p-values are statistically significant after correction because they are below the correction line [44].

4.3.4. Stratification by Baseline eGFR

There were 45 patients with eGFR less than 60 with an LLA, of which 62.2% (28/45) did not have AKI and 37.8% (17/45) had AKI. In this subpopulation, the no AKI group had a median AUC value of 28.1 mm Hg x hr (IQR 18.9, 38.6). The AKI group had a median of 27.8 mm Hg x hr (IQR 15.7, 51.3). The p-value of the rank-sum test was 0.35. The histograms of AUC values for the no AKI and AKI groups within the subpopulation of patients with eGFR less than 60 are

shown in Figure 21. The box plots for the AKI and no AKI groups in this subpopulation are

shown in Figure 22.

The logistic regression model for this high-risk patient group did not show an association

between AUC and AKI (OR 1.17 per 10 mm Hg x hr increase in AUC, 95% CI 0.82-1.68, p =

0.38).

Figure 21: Histograms of AUC for no AKI and AKI groups in subpopulation with eGFR less than 60. The p-value of the rank-sum test is shown above.
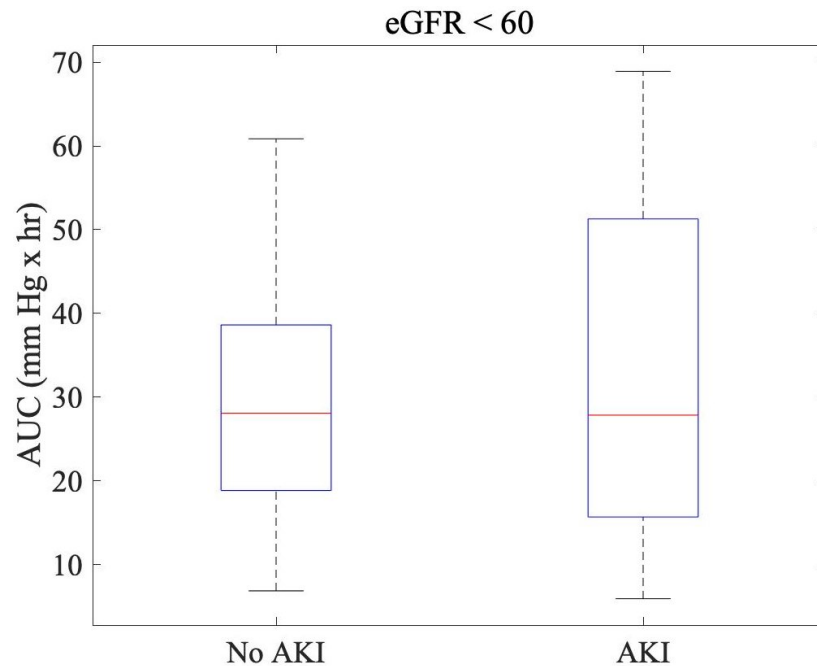
Figure 22: Box plots of AUC for no AKI and AKI groups in subpopulation with eGFR less than 60.

There were 117 patients with eGFR greater than 60 with an LLA, of which 93 did not have AKI and 24 had AKI. In this subpopulation, the no AKI group had a median AUC value of 23.9 mm Hg x hr (IQR 15.2, 34.9), while the AKI group had a median of 29.8 mm Hg x hr (IQR 23.6, 40.4). The histograms of AUC values for the no AKI and AKI groups within the subpopulation of patients with eGFR greater than 60 are shown in Figure 23. The p-value of the rank-sum test was 0.010. The box plots for the AKI and no AKI groups in this subpopulation are shown in Figure 24.

In contrast to patients with baseline impaired kidney function, the 117 patient subpopulation with eGFR greater than 60 had an odds ratio for AKI of 1.45 per 10 mm Hg x hr increase in AUC (95% CI 1.06-1.99, p = 0.022). This represents an increase in the odds of AKI

by a factor of about 9.21 as AUC increases from the minimum value to the maximum value in this subpopulation.

The statistical analyses on subpopulations with similar baseline kidney function suggested a lack of association between AUC and AKI in patients with compromised kidney function and a strong association in patients with healthy kidney function.
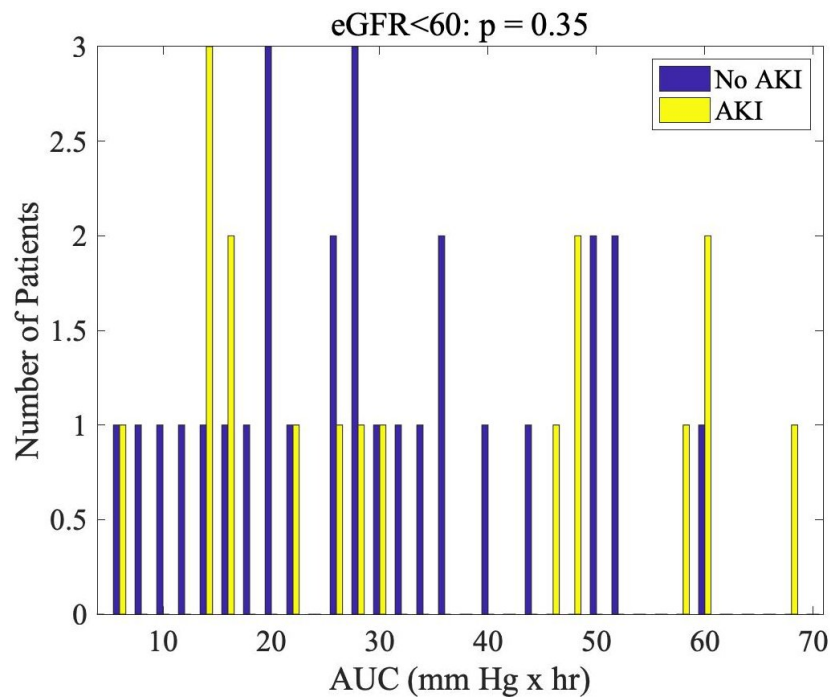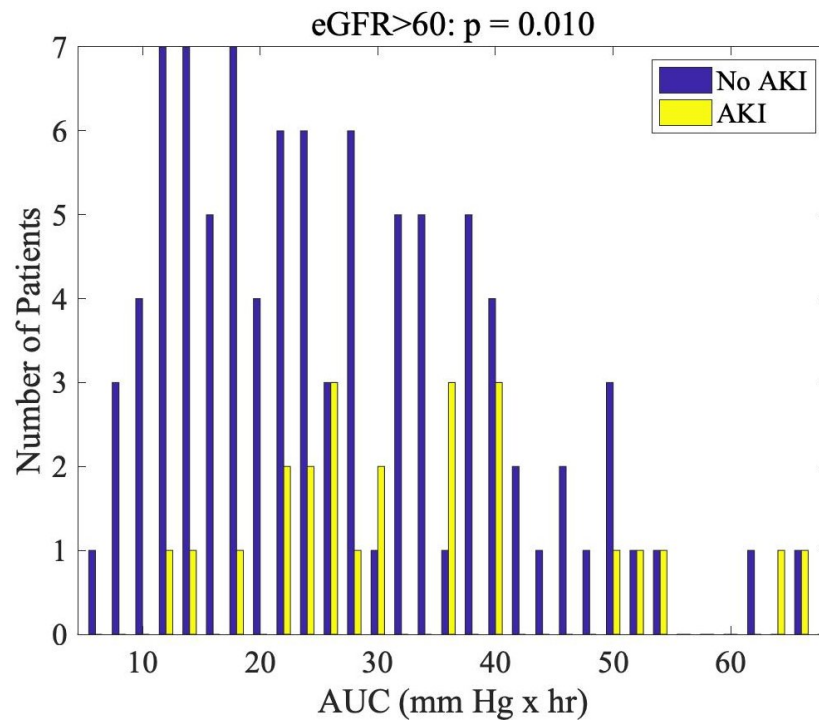

Figure 23: Histograms of AUC for no AKI and AKI groups in subpopulation with eGFR greater than 60. The p-value of the rank-sum test is shown above.
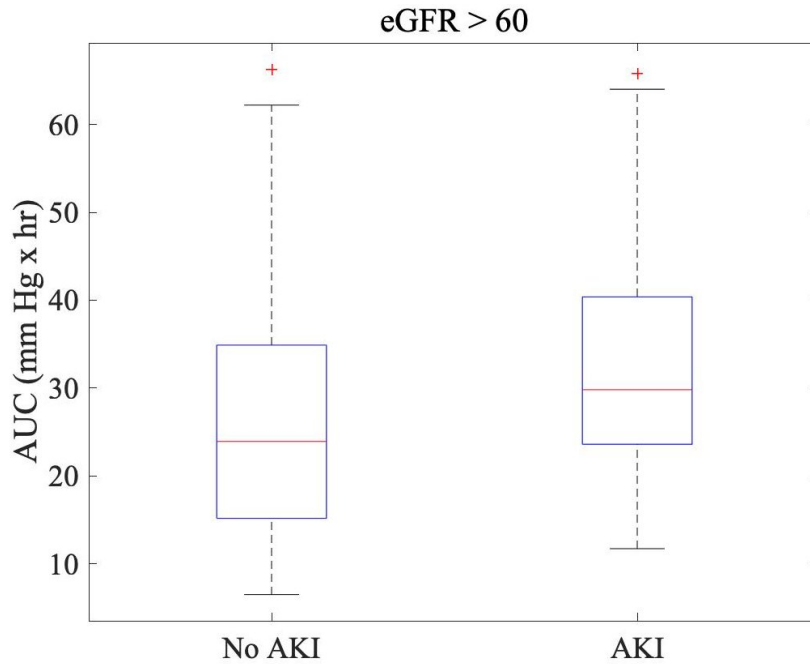
Figure 24: Box plots of AUC for no AKI and AKI groups in subpopulation with eGFR greater than 60.

4.4. Conclusions

The results presented in this chapter are intended to examine how the strength of association between ABP below the LLA and AKI changes with different parameter setting changes for this population. These findings are discussed below.

Time below LLA was found to have slightly greater statistical significance than AUC when testing for a higher median value of the measure of ABP below the LLA in the AKI group. However, it was also found to have less statistical significance as a predictor variable in logistic regression, although it did provide a slightly higher area under the ROC curve. Despite these mixed results, both time below LLA and AUC provided statistical significance in rank-sum

analysis and as predictors in logistic regression, which suggests that the two measures of ABP below the LLA are worth using in parallel in future research.

In choosing a COx threshold, there are several considerations. Ideally, the mean odds ratio would be maximized, the p-value from logistic regression would be minimized, and the number of patients without an LLA would be minimized. Although there were two clusters with relatively high odds ratios and low p-values, one from COx thresholds 0.125 through 0.15 and the other from COx thresholds 0.325 through 0.4, the cluster from 0.325 through 0.4 was considered more reliable because it was consistent with the COx threshold selection of approximately 0.3 obtained from prior research in both pigs and humans [16, 22]. A COx threshold of 0.325 is the most likely to be recommended for future use because it provided an LLA to the maximum number of patients among all threshold values in this cluster. It is worth mentioning that the odds ratio per 10 mm Hg x hr increase in AUC was between 1 and 1.7 at all 17 COx threshold values. This means that the percent increase in the odds of AKI for every increase of 10 mm Hg x hr in AUC was always below 70%. This can be accounted for by the fact that the overlap between the AKI and no AKI distributions was so large that the logistic regression model assigned a low probability of AKI to nearly all AUC values, as observed at a COx threshold of 0.3.

Each of the two subpopulations of patients with similar baseline kidney function provided vastly different results. Contrary to our prior hypothesis, the subpopulation with eGFR less than 60 did not show an association between AUC and AKI. This result may be caused by low sample size and imprecise results. Additionally, the distribution of AUC appeared higher than in the general population. One potential explanation for these results is that patients with kidney failure

often have vascular disease, leading to hemodynamic instability during surgery [45]. Additionally, it may be true that patients with low baseline kidney function are so vulnerable to any renal insult that ABP below the LLA is not a significant factor in determining their outcome. Regardless, these results did not support an association between AUC and AKI in this subpopulation. For the subpopulation with eGFR greater than 60, we found the strongest statistical significance for the association between AUC and AKI at a COx threshold of 0.3. Additionally, there were no patients in this subpopulation with an AUC of 10 mm Hg x hr or lower who developed AKI. These results imply that hypotension may be a significant factor in determining outcome for patients with healthy kidneys, and that blood pressure is therefore an important factor to optimize in these patients.

There are multiple limitations to this work that should be discussed. One of these is the low odds ratio values for both time below LLA and AUC. These suggest that this data is not conducive to high binary classification accuracy. The fact that more than half of patients did not have an LLA is another concern that needs to be addressed in future work in order to generalize these results to more patients. Since AKI is not diagnosed in patients who already have end-stage kidney failure, future stratified analysis should exclude these patients. Finally, the subpopulation with eGFR less than 60 had much fewer patients than is desirable for the statistical tests performed. Therefore, these tests should be repeated in a much larger patient population or in a study that addresses the issue of lack of an LLA for many patients.

Chapter 5

Discussion

5.1. Overview

In this thesis, we presented several methods and results related to the association between ABP below the LLA and acute kidney injury (AKI) in cardiac surgery. The initial step was to develop and test a MATLAB algorithm for rapid, automated LLA selection from COx error bar plots. With this algorithm, the ability to reproduce the association between area of the ABP curve below the LLA (AUC) and AKI found by Ono et al. was assessed in a new population of patients [1]. In addition, exploratory analyses were performed to search for stronger associations with slight variation in autoregulation analysis methods. The results obtained have substantial implications for both the viability of algorithmic approaches and the potential for autoregulation research to advance efforts in the prevention of perioperative AKI. But there are also several concerns that provide clear signals about which aspects of this research require further exploration. All of these elements of the significance of this work are discussed in this chapter.

5.2. Crucial Findings

5.2.1. Evaluation of Algorithmic LLA Selection

The algorithm utilized in this thesis implemented two methods of LLA selection. Each method had its unique purpose. Therefore, these two methods were validated against an expert clinician's

LLA selections separately, and the findings of each validation analysis have their own distinct implications for the value of algorithmic LLA selection approaches.

The primary method of algorithmic LLA selection, the threshold crossing method, was designed to imitate the traditional method of an expert clinician's LLA selections from COx error bar plots. When compared with expert selections, this method was found to have high agreement on both the presence or absence of an LLA in a plot and on the value of the LLA when it was present. This result is a promising indicator that an algorithm for LLA selection could be a valuable tool in autoregulation research. The use of an algorithm allows the creation of COx error bar plots, the selection of an LLA for each plot, and analysis of associations between ABP below the LLA and outcomes for all patients with an LLA to be performed within minutes by simply running one script file. This is in stark contrast to prior methods, in which some steps were automated but others, including LLA selection, involved careful inspection by clinicians. This increase in efficiency makes it more feasible to increase cohort size in future autoregulation studies. Furthermore, since an LLA selection method very similar to that of trained experts is built into the algorithm, autoregulation research may no longer be limited to research teams that are familiar with analyzing COx error bar plots.

The secondary method of algorithmic LLA selection, the parabola fit method, was designed to provide an LLA for certain COx error bar plots that do not have a threshold crossing but have a trend in mean COx values that resembles a parabola with a positive quadratic coefficient. This approach, which followed prior methods, was to fit a parabola to the mean COx values of such plots and estimate the LLA based on where this parabola crosses the threshold line [30, 31, 32]. If found to be useful, this method would be implemented at the same time as the

threshold crossing method so that autoregulation analysis results could be generalized to a much greater number of patients. Based on this goal, there are two important components to the viability of the parabola fit method: accuracy of LLA selection and assignment of an LLA to a significant number of patients who would not otherwise have one. The results of Chapter 2 demonstrated that this method assigned an LLA to a substantial minority of plots without a threshold crossing. Unfortunately, accuracy of the parabola fit method could not be fully evaluated in data from humans, as the gold standard for LLA selection in COx error bar plots is expert clinician selections by threshold crossing. When using this gold standard for validation, we found high agreement between expert clinician and parabola fit selections. However, we were not able to validate the parabola fit results in patients without an LLA from expert adjudication. Although these results do not truly validate the parabola fit method, they do suggest that the plot selection criteria for this method are reasonable. However, in order to closely follow the methods of prior autoregulation research and avoid drawing conclusions with unvalidated approaches, only the threshold crossing method of algorithmic LLA selection was used in Chapters 3 and 4. The results of analyses that used both methods of algorithmic LLA selection are included in Appendices A and B.

5.2.2. Analysis of Association to AKI

Once the algorithm's threshold crossing method was deemed to be a viable approach for LLA selection, this method was used to analyze associations between ABP below the LLA and AKI in a clinical cohort. The first step was to determine if these methods could reproduce the results of Ono et al. that found AUC to be associated with AKI [1]. With data from 345 patients from

cohorts between 2016 and 2019, a rank-sum test indicated that patients with AKI have a greater median value of AUC (mm Hg x hr) than patients without AKI. This result was consistent with prior findings [1]. The ability to find this association in a recent cohort of patients was significant, as the criteria for diagnosing AKI, methods of surgeons and anesthesiologists, types of procedures performed, and anesthetic medications used have all changed since the publication of Ono et al.'s research [9, 28, 29, 34, 35]. The existence of this association in the cohort used for this thesis implies that autoregulation analysis could potentially help prevent perioperative AKI in the future by allowing clinicians to target each patient's blood pressure above their own LLA. However, several additional studies are needed to establish this as a standard practice in the clinical setting.

After reproducing the association between AUC and AKI, the algorithm was used to evaluate the potential for slight variations in methods to produce a stronger association in this patient population. This was done by using time below LLA instead of AUC, varying the COx threshold, and stratifying by baseline kidney function as defined by eGFR. The effect of each of these modifications was assessed in isolation. This analysis revealed that time below LLA has a comparably strong association with AKI as AUC does, and that COx thresholds between 0.325 and 0.4 provide the strongest associations between AUC and AKI. In particular, a COx threshold of 0.325 appeared to be a suitable choice for maximizing the strength of association between AUC and AKI while attempting to minimize the number of patients without an LLA. In stratified analysis with rank-sum, the association between AUC and AKI was very weak when looking only at patients with severely compromised kidney function (eGFR less than 60), but even stronger than in non-stratified analysis when looking only at patients with kidney function that is

65

normal or slightly reduced (eGFR greater than 60) [41]. The results with eGFR greater than 60 provided particularly promising indicators that avoiding excursions of ABP below the LLA can be effective in preventing AKI. In addition to providing a statistically significant rank-sum test, this stratification significantly reduced the proportion of AKI patients with a low AUC. This suggests that in a population of patients with healthy kidney function, setting a target value for maximum tolerable AUC may be an effective strategy to prevent AKI during surgery. Future studies that focus on this patient population will be critical in deciding if such practices are sound.

5.3. Limitations and Future Directions

The methods and results in this thesis have notable implications for the future of autoregulation research, but also raise some concerns that merit further examination. Future work that addresses the limitations of this thesis and builds on its progress will be valuable in efforts to prevent AKI during surgery.

5.3.1. Algorithmic LLA Selection by Threshold Crossing

The accurate reproduction of expert LLA selection by threshold crossing with an algorithm was a significant development from this research. Widespread implementation of this algorithm would provide several advantages, including automation of nearly all steps required to examine associations with outcomes and well-defined, consistent methods. The improvement in efficiency of autoregulation analysis provided by an algorithm can be particularly advantageous in studies

involving 1000 or more patients. Furthermore, the algorithm's traits make it appropriate for use in multi-center autoregulation studies, for which it is critical to ensure that there are no discrepancies in signal processing steps, LLA selection methods, and analytic approaches between institutions. These examples illustrate the value that an algorithm can provide in large-scale, collaborative autoregulation research.

5.3.2. Algorithmic LLA Selection by Curve Fit

The accuracy of both the threshold crossing method and the parabola fit method of algorithmic LLA selection were evaluated by comparing the selections from these methods to those of an expert clinician. Since the algorithm's threshold crossing method is meant to reproduce the experts' method, the validation for this algorithmic method is not highly problematic.

Unfortunately, the same is not true when using expert LLA selection to validate the algorithm's parabola fit method of LLA selection. The parabola fit method is meant to provide an LLA for plots that do not have a threshold crossing. But since there are no expert selections of an LLA in such plots, the parabola fit LLA selections were instead evaluated in plots that have a threshold crossing. Although there was significant agreement between parabola fit and expert selections in this evaluation, this does not necessarily mean that the parabola fit method is accurate in plots that do not have a threshold crossing.

In addition to validation flaws for LLA selections, inability to select an LLA was a major issue. While the algorithm's threshold crossing method revealed statistically significant associations between ABP below the LLA and AKI, it did so while assigning an LLA to less than half of the patients in the study. The primary reason for this phenomenon is that more than half of

the COx error bar plots did not have a crossing from above to below the threshold line before the rightmost bin. This is a concerning result that prevents findings of autoregulation analysis from being generalized to all patients. Incorporating the parabola fit method for plots without a threshold crossing did reduce the scale of this problem, but roughly 40% of plots still did not have an LLA. This is largely explained by the fact that use of a parabola to estimate the LLA can only provide an LLA for the subset of plots that do not have an LLA, have all mean COx values below the threshold line, and have a parabolic trend in mean COx values. Thus, other methods are necessary to estimate the LLA for patients whose plots do not meet these criteria.

Research that explores methods for accurate LLA prediction in plots without a threshold crossing can be performed with robust validation in animal models. Since this data would contain true gold standard LLA values from scatter plots of laser-Doppler flux versus cerebral perfusion pressure, it would allow methods for curve fit LLA selection to be validated more rigorously [16]. With the ability to check all LLA selections against a true gold standard, a variety of curve fitting approaches can be implemented to determine how to maximize both LLA selection accuracy and number of LLA selections.

5.3.3. Targeting an Appropriate Patient Population

The results in this thesis showed an association between ABP below the LLA and AKI, but also demonstrated that the overlap in distributions of measures of ABP below the LLA between no AKI and AKI groups was too high to allow for accurate prediction models to be built. This is indicative of the fact that there are several factors that contribute to the risk of developing AKI

during surgery. These factors must be taken into account in order to thoroughly evaluate the value of autoregulation monitoring in efforts to prevent perioperative AKI.

In this thesis, baseline kidney function was the only additional variable accounted for when analyzing the strength of association between ABP below the LLA and AKI. However, there are several other conditions that may affect this association, including age, concomitant nephrotoxic drugs (i.e. IV contrast administration), or duration of cardiopulmonary bypass during surgery [2, 12]. Using these variables for stratification and multivariate modeling would provide more information about the true association between ABP below the LLA and AKI [46]. These analyses could reveal particular patient populations in which targeting ABP above the LLA is especially important, and would ensure that future surgical practices are not influenced by spurious associations [46].

5.4. Conclusions

This thesis discussed new tools that we developed for automated autoregulation analysis and presented analyses of the association between ABP below the LLA and AKI that utilized these tools. This work provided promising indicators that autoregulation monitoring could be valuable in preventing AKI, but needs validation in studies that incorporate a variety of additional analyses. Augmenting this future work with the tools from this thesis could help accelerate the implementation of autoregulation monitoring as a guide for improving surgical outcomes.

Appendix A

Demonstrating an Association of AUC with Acute Kidney Injury Using Threshold Crossing and Parabola Fit Methods of LLA Selection

A.1. Introduction

In Chapter 3, the association of AUC with AKI was demonstrated in a cohort of patients using the threshold crossing method to select the LLA, since this method was validated in Chapter 2 [1]. Although a parabola fit method was also developed, it could not be fully validated in humans due to lack of a reference standard in cases in which an expert LLA could not be determined. Nevertheless, the results of Chapter 2 also demonstrated that in plots that have an LLA by expert selection, the parabola fit LLA values showed relatively small deviation from these selections. For this reason, this appendix presents the ability to reproduce the association between AUC and

AKI when using both the threshold crossing method and the parabola fit method of algorithmic LLA selection.

A.2. Methods

The patient population, method of calculating AUC, definition of AKI, and analytic approaches in this appendix were identical to those of Chapter 3. However, in this appendix, LLA values were selected by the threshold crossing method whenever possible, or by the parabola fit method when available in plots without a threshold crossing.

A.3. Results

Implementation of the parabola fit method gave an LLA to 44 additional patients, so that an LLA was available for 206 patients in this analysis. Out of these patients, the incidence of AKI was 22.8% (47/206). The group of patients who did not have AKI had a mean LLA of 76.2 mm Hg and a mean baseline SCr of 1.2 mg/dL, while the group of patients who had AKI had a mean LLA of 73.9 mm Hg and a mean baseline SCr of 1.3 mg/dL. The combined distribution of AUC values for these 206 patients had a median AUC of 21.6 mm Hg x hr (IQR 11.4, 33.8). The histograms of AUC for the no AKI and AKI groups are shown in Figure 25.
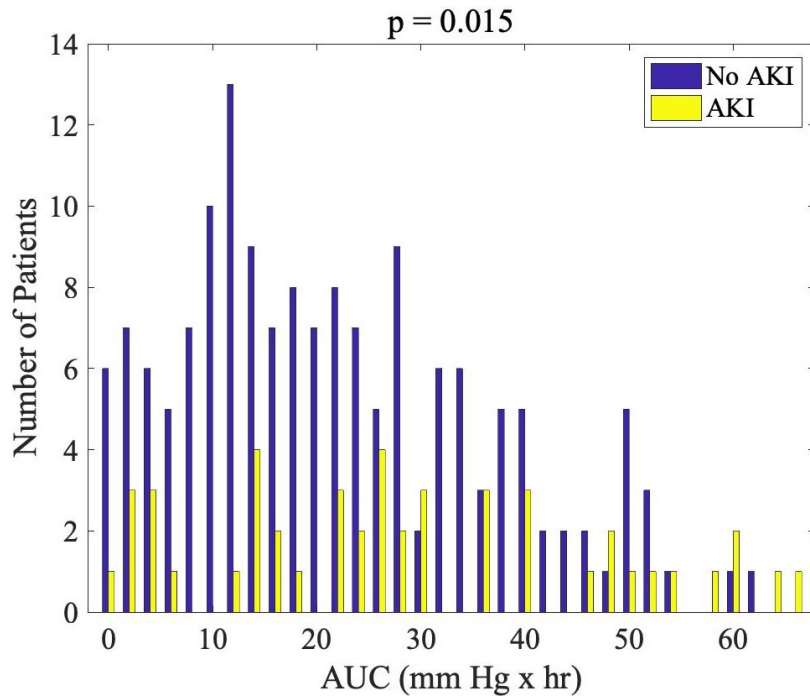
Figure 25: Histograms of AUC for no AKI and AKI groups when using both methods of LLA selection. The p-value of the rank-sum test is shown above.
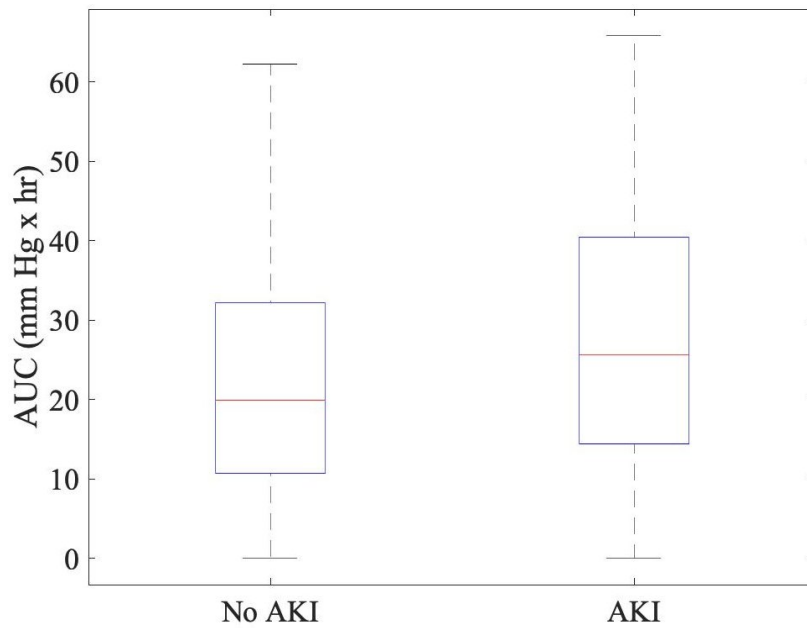

Figure 26: Box plots of AUC for no AKI and AKI groups when using both methods of LLA selection.

Figure 26 shows the box plot distribution of AUC by AKI status.The median, 25th

percentile, and 75th percentile values of AUC were all higher in patients with AKI, who had a

median of 25.6 mm Hg x hr (IQR 14.4, 40.4) compared with patients without AKI, who had a

median of 19.9 mm Hg x hr (IQR 10.7, 32.2). The rank-sum test returned a p-value of 0.015.

The logistic regression model returned an odds ratio of 1.29 per 10 mm Hg x hr increase

in AUC, with a 95% confidence interval of 1.06-1.58 and a p-value of 0.013. This odds ratio

represents an increase in odds of AKI by a factor of 5.44 as AUC increases from the minimum

value to the maximum value in this population.

A.4. Conclusions

This appendix demonstrated an association between AUC and AKI when an additional 44

patients with an LLA selected by parabola fit were included in analysis. Although this addition

reduced the odds ratio, p-values remained about the same, so that the association remained

statistically significant at the 5% level.

While there was an association between AUC and AKI when incorporating the parabola

fit method, the additional patients drastically affected the distribution of AUC values. Since the

median, 25th percentile, and 75th percentile values for AUC in both the AKI and no AKI groups

were much lower after patients with a parabola fit LLA were incorporated, it is clear that this

method tends to produce very low AUC values. It is certainly plausible that patients with a

parabola fit LLA experience did not experience significant excursions of ABP below the LLA, as

the parabola fit method is used in plots with all mean COx values below 0.3, a condition that

73

indicates intact autoregulation,. However, since this method is not validated, it is also possible that it tends to underestimate the LLA.

The effect of incorporating parabola fit LLA patients on the AUC distributions of the no AKI and AKI groups may provide some clues about the validity of this method, but it is also important to examine the ability of this method to increase sample size. With the threshold crossing and parabola fit methods implemented, about 40% of patients did not have an LLA. This is significantly lower than the 53% without an LLA when only the threshold crossing method was used. However, this result also suggests that other approaches are needed to maximize the number of patients with an LLA.

Appendix B

Sensitivity Analyses Using Threshold Crossing and Parabola Fit Methods of LLA Selection

B.1. Introduction

In Appendix A, we demonstrated an association between AUC and AKI using a cohort of patients in which the LLA was determined by both threshold crossing and parabola fit methods. In Appendix B we expand this work by presenting sensitivity analyses using the same cohort of patients. The sensitivity analyses are identical to those in Chapter 4 and are use of time below LLA instead of AUC, varying the COx threshold, and stratification by baseline kidney function.

B.2. Methods

The patient population, methods of calculating AUC and time below LLA, definition of AKI, method of stratifying by baseline kidney function, and analytic plan in this appendix were the same as in Chapter 4. LLA values were selected by the threshold crossing method whenever possible. Among plots without an LLA by threshold crossing, those that met the criteria

described in Chapter 2 had an LLA selected by the parabola fit method. The ROC curve of the logistic regression model for time below LLA was compared to the ROC curve of the logistic regression model for AUC discussed in Appendix A.

B.3. Results

B.3.1. Use of Time Below LLA

Implementation of the parabola fit method at a COx threshold of 0.3 gave an LLA to 44 additional patients, so that an LLA was available for 206 patients in this analysis. The incidence of AKI among these patients was 22.3% (46/206). For the no AKI group, the median value of time below LLA was 3.0 hr (IQR 2.2, 3.8). For the AKI group, the median value of time below LLA was 3.7 hr (IQR 2.6, 4.4). The p-value of the one-tailed rank-sum test was 0.0086. Figure 27 shows histograms for these time below LLA distributions with a bin size of 0.25 hr. Figure 28 contains box plots of the distribution of time below LLA values for the no AKI and AKI groups.
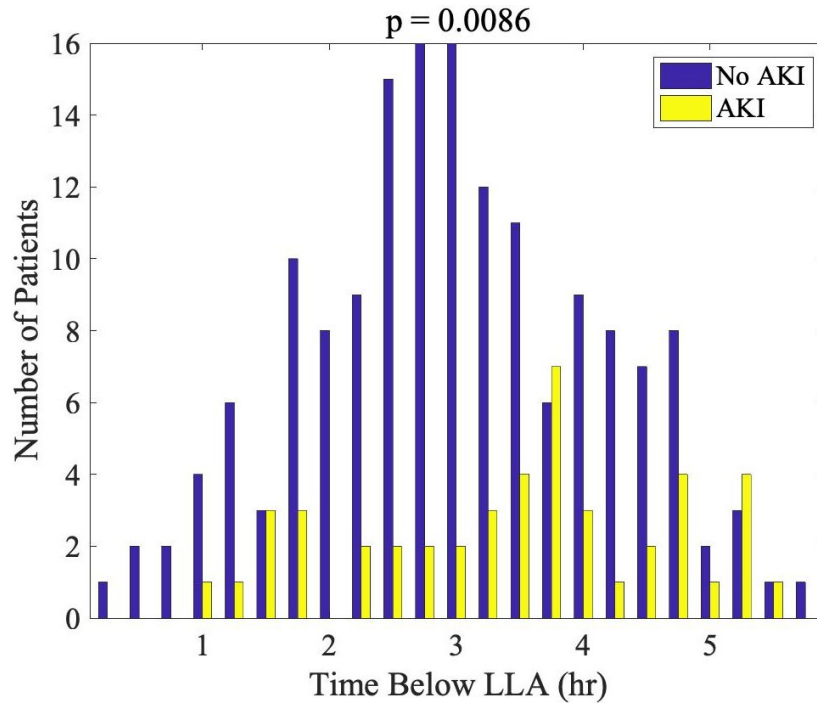
Figure 27: Histograms of time below LLA for no AKI and AKI groups when using both methods of LLA selection. The p-value of the rank-sum test is shown above.
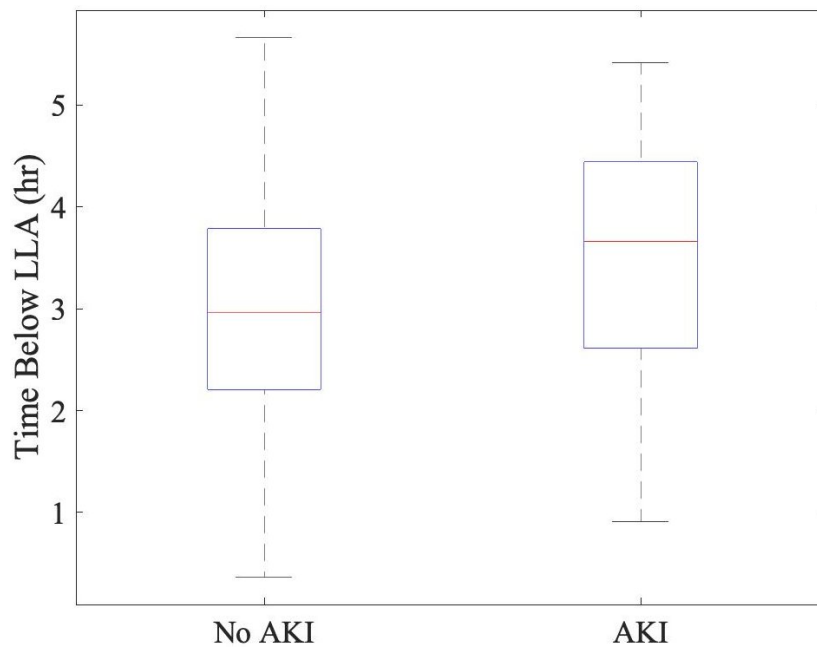
Figure 28: Box plots of time below LLA for no AKI and AKI groups when using both methods of LLA selection.

The logistic regression model returned an odds ratio of 1.42 per 1 hr increase in time below LLA, with a 95% confidence interval of 1.06-1.90 and a p-value of 0.018. This odds ratio represents an increase in the odds of AKI by a factor of about 6.41 as time below LLA increases from the minimum to the maximum value in this population.

The ROC curves for AUC and time below LLA at a COx threshold of 0.3 are shown in Figure 29. The area under the ROC curve for AUC was 0.605, and the area under the ROC curve for time below LLA was 0.615. Both logistic regression models did not assign a probability of AKI greater than 0.5 to any of the 206 patients.

In these results, time below LLA and AUC at a COx threshold of 0.3 showed comparable strengths of association with AKI.

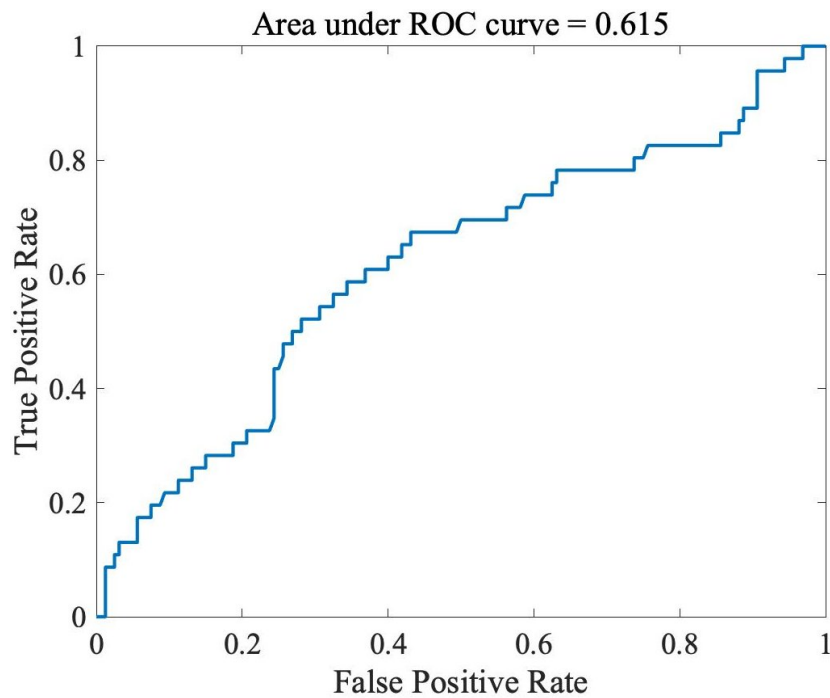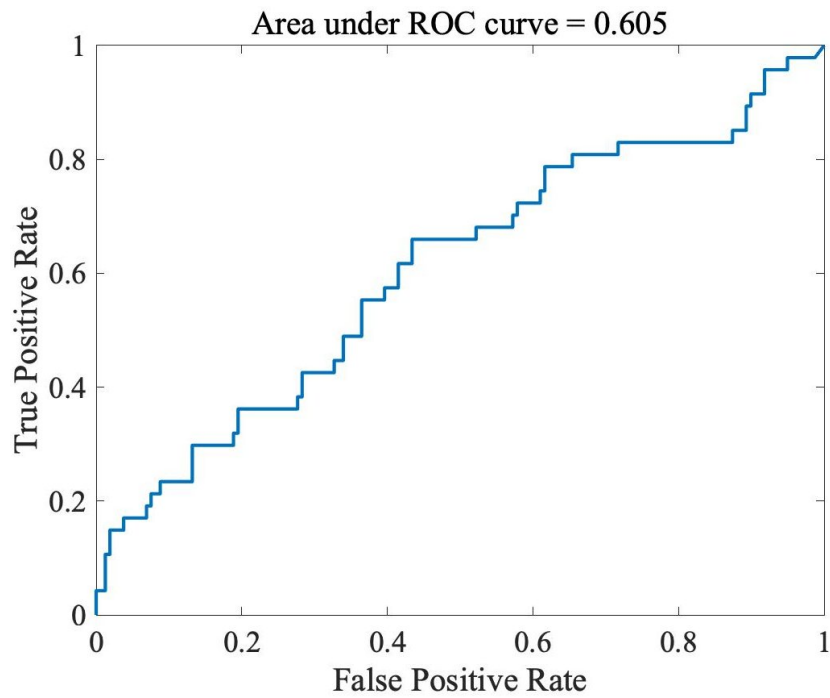**Figure 29: ROC curves at a COx threshold of 0.3 when using both methods of LLA selection. The top curve was generated with AUC as the predictor variable, and the bottom curve used time below LLA. The area under each ROC curve is shown above.**

B.3.2. Varying the COx Threshold

Table 4 shows the outputs of logistic regression models with AUC as the predictor variable that estimate the odds of AKI at each COx threshold, as well as the number of patients with an LLA (excluding outliers) at each threshold. These results reveal a cluster from COx thresholds 0.35 through 0.45 that contains the five highest odds ratios and five lowest p-values among all of the COx thresholds used. The highest odds ratio and lowest p-value are observed at a COx threshold of 0.375. This threshold value provided an LLA for 57.1% (197/345) of patients, compared with the maximum of 60.6% (209/345) patients with an LLA achieved at a COx threshold of 0.325. Figure 30 shows multiple comparison correction of these p-values with the Benjamini-Yekutieli procedure at 5% significance. The six lowest p-values were below the line, and therefore remained statistically significant after multiple comparison correction [44]. These p-values occurred at COx thresholds of 0.275 and 0.35 through 0.45.

In these results, there was one distinct cluster from COx thresholds 0.35 through 0.45 at which the association between AUC and AKI was the strongest. Within this cluster, a COx threshold of 0.375 was clearly the optimal value, as it maximized number of patients with an LLA and odds ratio while minimizing p-value.

COx threshold	Odds ratio (OR)	95% CI	p-value	Number of patients with an LLA
0.1	1.18	0.91-1.53	0.207	133
0.125	1.38	1.08-1.78	0.011	151
0.15	1.30	1.04-1.62	0.023	166
0.175	1.31	1.07-1.60	8.44×10^{-3}	171
0.2	1.27	1.03-1.57	0.027	176
0.225	1.24	1.03-1.49	0.026	190
0.25	1.30	1.06-1.59	0.011	198
0.275	1.38	1.12-1.69	2.19×10^{-3}	200
0.3	1.29	1.06-1.58	0.013	206
0.325	1.29	1.07-1.56	8.63×10^{-3}	209
0.35	**1.40**	**1.14-1.72**	**1.14×10^{-3}**	**194**
0.375	**1.52**	**1.23-1.88**	**8.56×10^{-5}**	**197**
0.4	**1.49**	**1.19-1.87**	**4.45×10^{-4}**	**195**
0.425	**1.44**	**1.14-1.81**	**2.04×10^{-3}**	**192**
0.45	**1.47**	**1.15-1.86**	**1.73×10^{-3}**	**186**
0.475	1.31	1.01-1.71	0.044	176
0.5	1.16	0.88-1.55	0.292	162

Table 4: Statistics for logistic regression with AUC as predictor of AKI at 17 different COx threshold values when using both methods of LLA selection. Statistics reported include odds ratio per 10 mm Hg x hr increase in AUC and its 95 percent confidence interval, p-value of AUC in logistic regression, and number of patients with an LLA.
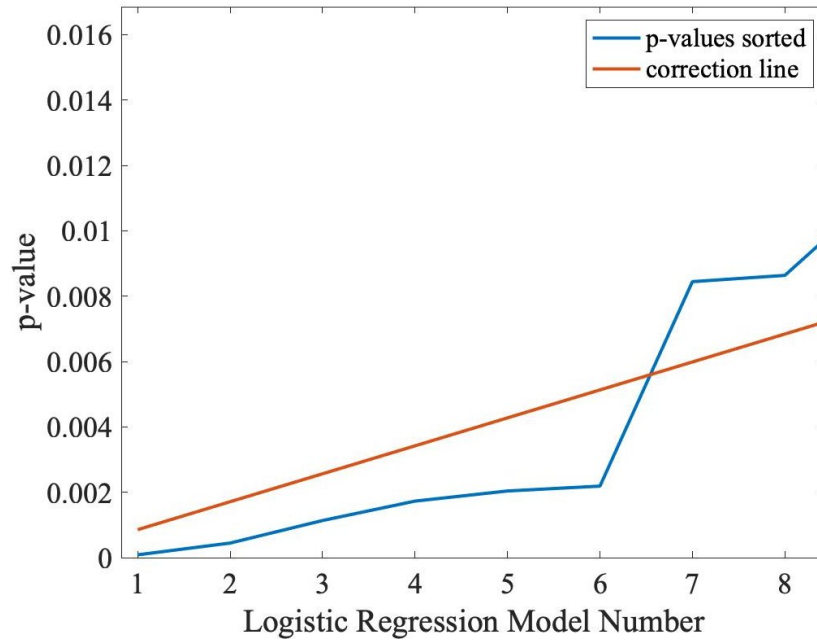
Figure 30: Multiple comparison correction of p-values from logistic regression by the Benjamini-Yekutieli procedure at 5 percent significance when using both methods of LLA selection. Logistic regression models are sorted in order of increasing p-value, and the plot is zoomed in on the eight lowest p-values. The six lowest p-values are statistically significant after correction because they are below the correction line [44].

B.3.3. Stratification by Baseline eGFR

Of the 44 patients with an LLA by parabola fit at a COx threshold of 0.3, 7 had an eGFR less than 60. Therefore, the subpopulation of patients with eGFR less than 60 grew to 52 patients, with an incidence of AKI of 30.8% (16/52). In this subpopulation, the no AKI group had a median AUC value of 20.8 mm Hg x hr (IQR 11.8, 35.1). The AKI group had a median of 26.4 mm Hg x hr (IQR 15.4, 48.6). The p-value of the rank-sum test was 0.11. The histograms of AUC values for the no AKI and AKI groups within the subpopulation of patients with eGFR less

than 60 are shown in Figure 31. The box plots of the AKI and no AKI groups for this

subpopulation are shown in Figure 32.

The logistic regression model for this 52 patient subpopulation with eGFR less than 60

did not show an association between AUC and AKI (OR 1.29 per 10 mm Hg x hr increase in
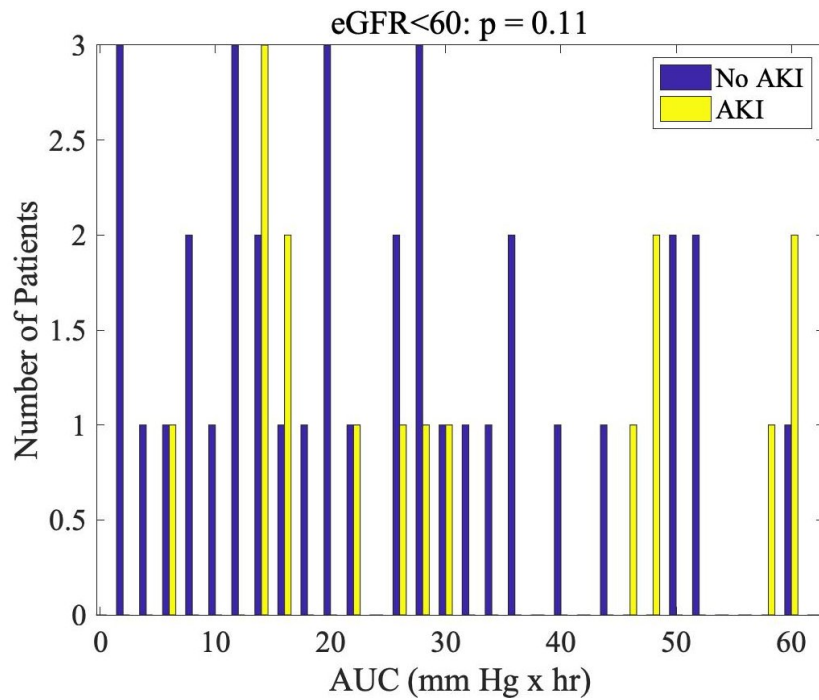
AUC, 95% CI 0.91-1.82, p = 0.16).

Figure 31: Histograms of AUC for no AKI and AKI groups in subpopulation with eGFR

less than 60 when using both methods of LLA selection. The p-value of the rank-sum test is
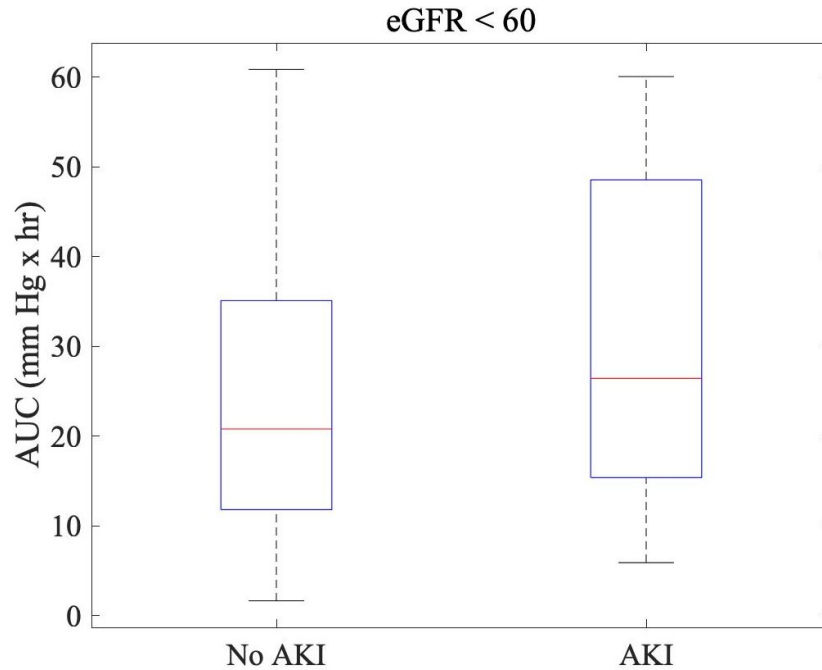
shown above.

Figure 32: Box plots of AUC for no AKI and AKI groups in subpopulation with eGFR less than 60 when using both methods of LLA selection.

Of the 44 patients with an LLA by parabola fit at a COx threshold of 0.3, 37 had an eGFR greater than 60. Therefore, the subpopulation of patients with eGFR greater than 60 grew to 154 patients, with an incidence of AKI of 20.1% (31/154). In this subpopulation, the no AKI group had a median AUC value of 18.1 mm Hg x hr (IQR 10.5, 31.2), while the AKI group had a median of 25.6 mm Hg x hr (IQR 12.3, 39.0). The histograms of AUC values for the no AKI and AKI groups within the subpopulation of patients with eGFR greater than 60 are shown in Figure 33. The p-value of the rank-sum test was 0.056. The box plots of the AKI and no AKI groups for this subpopulation are shown in Figure 34.

The logistic regression model for the 154 patient subpopulation with eGFR greater than 60 also did not show an association between AUC and AKI (OR 1.27 per 10 mm Hg x hr

increase in AUC, 95% CI 0.99-1.63, p = 0.065). This odds ratio represents an increase in the

odds of AKI by a factor of 4.78 as AUC increases from the minimum to the maximum value in

this subpopulation.

These statistical analyses involving eGFR stratification suggested a lack of association

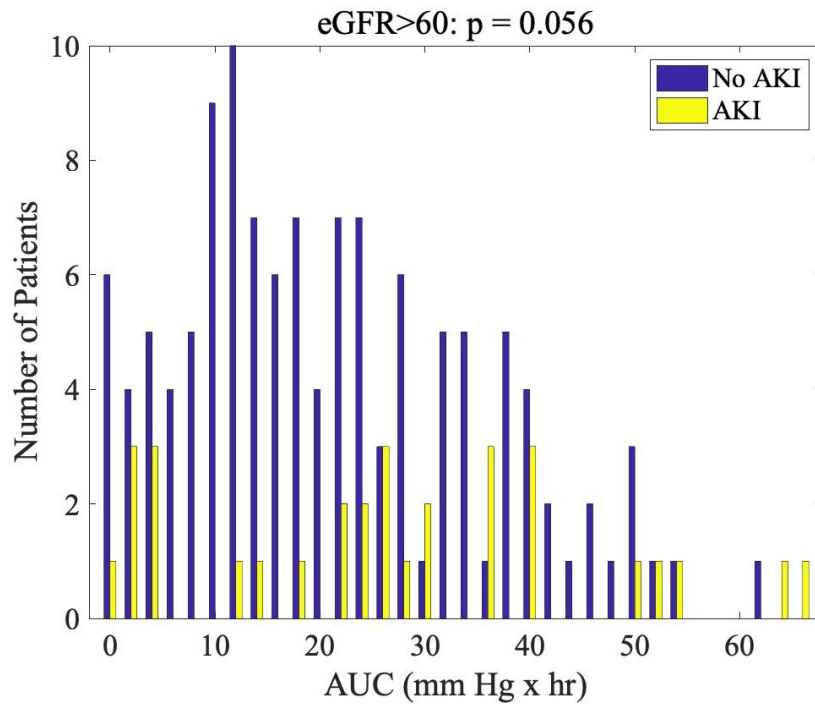between AUC and AKI in both subpopulations of patients with similar baseline kidney function.

Figure 33: Histograms of AUC for no AKI and AKI groups in subpopulation with eGFR greater than 60 when using both methods of LLA selection. The p-value of the rank-sum test is shown above.
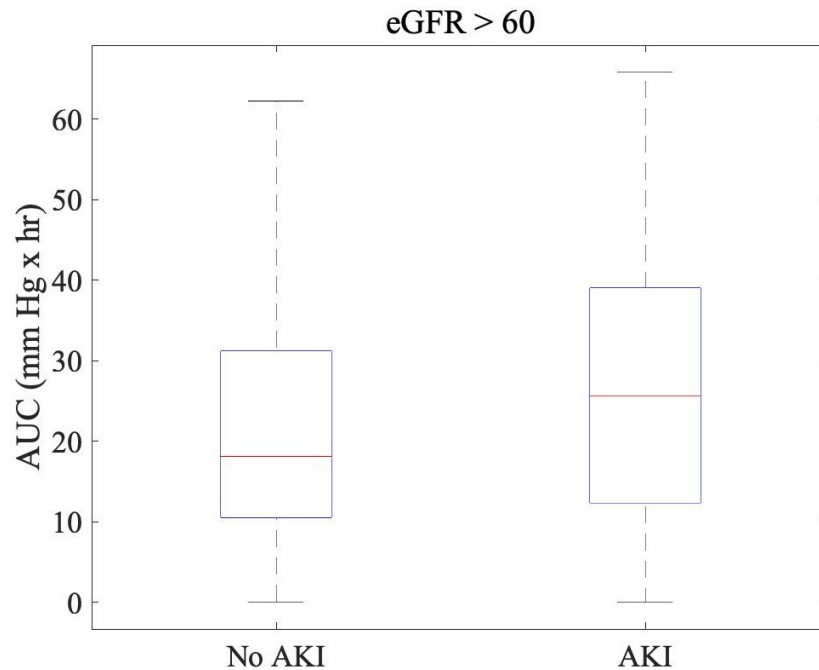
Figure 34: Box plots of AUC for no AKI and AKI groups in subpopulation with eGFR greater than 60 when using both methods of LLA selection.

B.4. Conclusions

The results in this appendix demonstrated that the addition of patients with an LLA by parabola fit had minimal impact on the findings of some sensitivity analyses but substantially altered others.

Incorporating parabola fit LLA patients did very little to change the conclusions about the choice of measure of ABP below the LLA that were observed in Chapter 4. For both AUC and time below LLA, adding these 44 patients had little effect on the strength of association with AKI. The p-values, odds ratios, and ROC curves obtained for AUC and time below LLA when both algorithmic methods of LLA selection were used suggested that both variables have an

association with AKI, but neither one is clearly a far superior predictor variable. This is consistent with the results from Chapter 4.

The results at different COx thresholds changed significantly with the addition of parabola fit LLA patients. This analysis provided a cluster of high odds ratios and low p-values from COx thresholds 0.35 through 0.45, and suggested that a COx threshold of 0.375 is the optimal choice for balancing the concerns of maximizing odds ratio, minimizing p-value, and maximizing the number of patients with an LLA. This finding is much less ambiguous than that observed in Chapter 4, in which COx thresholds of 0.375 and 0.4 provided a strong association between AUC and AKI but also excluded a significant number of patients. However, given that the parabola fit method has never been evaluated against gold standard LLA values, a COx threshold of 0.325 may be recommended for future use based on the results of Chapter 4, while a COx threshold of 0.375 would not be recommended in spite of the results in this appendix.

Incorporating the parabola fit LLA method also had a drastic effect on the results of stratification by baseline eGFR. In the subpopulation with eGFR less than 60, inclusion of these patients decreased the p-values from both rank-sum and logistic regression, but both of these remained above the 5% significance level. This decrease can be explained by the tendency of the parabola fit method to produce very low AUC values as well as the fact that all parabola fit LLA patients in this subpopulation did not have AKI. In spite of these effects of using the parabola fit method, this subpopulation showed no association between AUC and AKI, which is consistent with the findings of Chapter 4. In the subpopulation with eGFR greater than 60, incorporating parabola fit LLA patients gave results that suggested no association between AUC and AKI. This contradicts the results of Chapter 4, which found a stronger association between AUC and AKI in

87

this subpopulation than in a non-stratified population. This is likely due to low AUC values

produced by the parabola fit method that had a drastic effect on the distribution in the AKI group.

While this contradiction is not ideal, it does not justify a rejection of the findings from Chapter 4

in this subpopulation. The most important factor in determining the validity of these findings

would be the ability to reproduce them with only the threshold crossing method in other cohorts

of patients.

Bibliography

1. Ono M, Arnaoutakis GJ, Fine DM, et al. Blood pressure excursions below the cerebral autoregulation threshold during cardiac surgery are associated with acute kidney injury. *Crit Care Med*. 2013;41(2):464–471.

2. Mao H, Katz N, Ariyanon W, et al. Cardiac surgery-associated acute kidney injury. *Cardiorenal Med*. 2013;3(3):178–199.

3. Jilles B. Bijker, Wilton A. van Klei, Teus H. Kappen, Leo van Wolfswinkel, Karel G. M. Moons, Cor J. Kalkman; Incidence of Intraoperative Hypotension as a Function of the Chosen Definition: Literature Definitions Applied to a Retrospective Cohort Using Automated Data Collection. *Anesthesiology* 2007;107(2):213-220.

4. Zweifel C, Dias C, Smielewski P, et al. Continuous time-domain monitoring of cerebral autoregulation in neurocritical care. Med Eng Phys 2014; 36: 638–645.

5. Brady KM, Mytar JO, Lee JK, et al. Monitoring cerebral blood flow pressure autoregulation in pediatric patients during cardiac surgery. *Stroke*. 2010;41(9):1957–1962.

6. Acute kidney failure. Mayo Clinic. https://www.mayoclinic.org/diseases-conditions/kidney-failure/symptoms-causes/syc-20369048. Published June 23, 2018. Accessed April 29, 2019.

7. O'Neal JB, Shaw AD, Billings FT 4th. Acute kidney injury following cardiac surgery: current understanding and future directions. *Crit Care*. 2016;20(1):187. Published 2016 Jul 4.

8. Karkouti K, Wijeysundera DN, Yau TM, Callum JL, Cheng DC, Crowther M, et al. Acute kidney injury after cardiac surgery: focus on modifiable risk factors. Circulation. 2009;119(4):495–502.

9. Makris K, Spanou L. Acute Kidney Injury: Definition, Pathophysiology and Clinical Phenotypes. *Clin Biochem Rev*. 2016;37(2):85–98.

10. Yang F, Zhang L, Wu H, Zou H, Du Y. Clinical analysis of cause, treatment and prognosis in acute kidney injury patients. *PLoS One*. 2014;9(2):e85214. Published 2014 Feb 21. doi: 10.1371/journal.pone.0085214

11. Moore P. K., Hsu R. K., Liu K. D. Management of acute kidney injury: core curriculum 2018. *American Journal of Kidney Diseases*. 2018;72(1):136–148.

12. Meersch M, Schmidt C, Hoffmeier A, et al. Prevention of cardiac surgery-associated AKI by implementing the KDIGO guidelines in high risk patients identified by biomarkers: the PrevAKI randomized controlled trial [published correction appears in Intensive Care Med. 2017 Mar 7;:]. *Intensive Care Med*. 2017;43(11):1551–1561.

13. Cerebral Autoregulation. Cerebral Autoregulation - an overview. https://www.sciencedirect.com/topics/neuroscience/cerebral-autoregulation. Accessed April 29, 2019.

14. Fantini S, Sassaroli A, Tgavalekos KT, Kornbluth J. Cerebral blood flow and autoregulation: current measurement techniques and prospects for noninvasive optical methods. *Neurophotonics*. 2016;3(3):031411. doi:10.1117/1.NPh.3.3.031411

15. Rivera-Lara L, Zorrilla-Vaca A, et al. Determining the Upper and Lower Limits of Cerebral Autoregulation With Cerebral Oximetry Autoregulation Curves: A Case Series. *Crit Care Med.* 2019;46(5):473-477.

16. Brady KM, Lee JK, Kibler KK, et al. Continuous time-domain analysis of cerebrovascular autoregulation using near-infrared spectroscopy. *Stroke*. 2007;38(10):2818–2825.

17. Luo Z, Benveniste H, Yu M, Du C. Activation-Blood Flow Coupling During Direct Somatosensory Cortical Stimulation in Living Rat Brain. *IEEE*. 2005

18. Blaber A. P., Bondar R. L., Stein F., et al. Transfer function analysis of cerebral autoregulation dynamics in autonomic failure patients. *Stroke*. 1997;28(9):1686–1692.

19. Czonsnyka M., Brady K., Reinhard M., Smielewski P., Steiner L. Monitoring of cerebrovascular autoregulation: facts, myths, and missing links. *Neurocritical Care*. 2009;10(3):373–386.

20. Hori D, Brown C, Ono M, et al. Arterial pressure above the upper cerebral autoregulation limit during cardiopulmonary bypass is associated with postoperative delirium. *Br J Anaesth*. 2014;113(6):1009–1017.

21. Thewissen L, Caicedo A, Lemmers P, Van Bel F, Van Huffel S, Naulaers G. Measuring Near-Infrared Spectroscopy Derived Cerebral Autoregulation in Neonates: From Research Tool Toward Bedside Multimodal Monitoring. *Front Pediatr*. 2018;6:117. Published 2018 May 14.

22. Brady K, Joshi B, Zweifel C, et al. Real-time continuous monitoring of cerebral blood flow autoregulation using near-infrared spectroscopy in patients undergoing cardiopulmonary bypass. *Stroke*. 2010;41(9):1951–1956.

23. Kirsch J.D. (2016) Essentials of Transcranial Doppler Ultrasound. In: Saba L., Raz E. (eds) *Neurovascular Imaging.* Springer, New York, NY

24. Moerman A, De Hert S. Recent advances in cerebral oximetry. Assessment of cerebral autoregulation with near-infrared spectroscopy: myth or reality?. *F1000Res*. 2017;6:1615. Published 2017 Aug 31.

25. W Tosh, M Patteril, Cerebral oximetry. *BJA Education.* 2016;16(12):417–421

26. Troianos C. Cerebral Oximetry May Provide Helpful Information. *Anesthesia Patient Safety Foundation.* 2009;24(1):1-24.

27. Ono M, Brady K, Easley RB, et al. Duration and magnitude of blood pressure below cerebral autoregulation threshold during cardiopulmonary bypass is associated with major morbidity and operative mortality. *J Thorac Cardiovasc Surg*. 2013;147(1):483–489.

28. Prielipp RC, Cohen NH. The future of anesthesiology: implications of the changing healthcare environment. Curr Opin Anaesthesiol. 2016;29(2):198–205.

29. NHS Choices. http://www.nhs.uk/conditions/aortic-valve-replacement/alternatives/. Accessed April 29, 2019.

30. Zeiler FA, Czosnyka M, Smielewski P. Optimal cerebral perfusion pressure via transcranial Doppler in TBI: application of robotic technology. *Acta Neurochir (Wien)*. 2018;160(11): 2149–2157.

31. Aries MJ, Czosnyka M, Budohoski KP, et al. Continuous determination of optimal cerebral perfusion pressure in traumatic brain injury. Crit Care Med. 2012;40:2456–2463.

32. Liu X, Maurits NM, Aries MJH, et al. Monitoring of optimal cerebral perfusion pressure in traumatic brain injured patients using a multi-window weighting algorithm. J Neurotrauma. 2017;34(22):3081–3088.

33. Giavarina D. Understanding Bland Altman analysis. *Biochem Med (Zagreb)*. 2015;25(2): 141–151. Published 2015 Jun 5.

34. Mahmoud M, Mason KP. Recent advances in intravenous anesthesia and anesthetics. *F1000Res*. 2018;7:F1000 Faculty Rev-470. Published 2018 Apr 17.

35. Chitilian HV, Eckenhoff RG, Raines DE. Anesthetic drug development: Novel drugs and new approaches. *Surg Neurol Int*. 2013;4(Suppl 1):S2–S10. Published 2013 Mar 19.

36. Machado MN, Nakazone MA, Maia LN. Acute kidney injury based on KDIGO (Kidney Disease Improving Global Outcomes) criteria in patients with elevated baseline serum creatinine undergoing cardiac surgery. *Rev Bras Cir Cardiovasc*. 2014;29(3):299–307.

37. HOW DO I INTERPRET ODDS RATIOS IN LOGISTIC REGRESSION? UCLA Institute for Digital Research and Education. https://stats.idre.ucla.edu/stata/faq/how-do-i-interpret-odds-ratios-in-logistic-regression/. Accessed April 30, 2019.

38. SAS/STAT(R) 9.3 User's Guide. http://support.sas.com/documentation/cdl/en/statug/63962/HTML/default/viewer.htm#statug_logistic_sect040.htm. Published July 15, 2011. Accessed April 29, 2019.

39. There's Nothing Odd about the Odds Ratio: Interpreting Binary Logistic Regression. Statistics Solutions. http://www.statisticssolutions.com/theres-nothing-odd-about-the-odds-ratio-interpreting-binary-logistic-regression/. Published April 12, 2018. Accessed April 29, 2019.

40. Estimating Glomerular Filtration Rate. National Institute of Diabetes and Digestive and Kidney Diseases. https://www.niddk.nih.gov/health-information/communication-programs/nkdep/laboratory-evaluation/glomerular-filtration-rate/estimating. Accessed April 29, 2019.

41. Weinstein J. eGFR Calculator. UKidney's Nephrology Community. https://ukidney.com/nephrology-resources/egfr-calculator. Accessed April 29, 2019.

42. Zeiler FA, Ercole A, et al. Comparison of Performance of Different Optimal Cerebral Perfusion Pressure Parameters for Outcome Prediction in Adult Traumatic Brain Injury: A

Collaborative European NeuroTrauma Effectiveness Research in Traumatic Brain Injury (CENTER-TBI). *Journal of Neurotrauma.* 2018:1-13.

43. Basile DP, Anderson MD, Sutton TA. Pathophysiology of acute kidney injury. *Compr Physiol*. 2012;2(2):1303–1353.

44. Benjamini Y, Yekutieli D. The control of the false discovery rate in multiple testing under dependency. *Ann. Statist.* 2001;29(4):1165-1188.

45. Martens CR, Edwards DG. Peripheral vascular dysfunction in chronic kidney disease. *Cardiol Res Pract*. 2011;2011:267257.

46. Pourhoseingholi MA, Baghestani AR, Vahedi M. How to control confounding effects by statistical analysis. *Gastroenterol Hepatol Bed Bench*. 2012;5(2):79–83.

Curriculum Vitae

Rohan Nadkarni was born in September of 1994 in Illinois, USA.

When Rohan was 10 years old, his family moved to the San Francisco Bay Area, where he stayed for 5th grade through the end of high school. Rohan graduated from Monta Vista High School in Cupertino, California in June 2013.

In September 2013, Rohan began his undergraduate studies at the University of California, Los Angeles (UCLA). During his time at UCLA, he spent 22 months working in Aydogan Ozcan's research lab and spent 12 months working in Fabien Scalzo's research lab. For his Bioengineering capstone design course project, he worked with 5 other undergraduates to design a low-cost quantitative phase microscope that was meant to evaluate the efficacy of chemotherapeutics on cancer cells. He graduated from UCLA in June 2017 with a B.S. in Bioengineering.

In August 2017, Rohan began his graduate studies at Johns Hopkins University. He is enrolled in a Master's degree program in Biomedical Engineering.